ATAXIN-1 NUCLEAR BODIES

Ataxin-1 Nuclear Bodies are Subnuclear Sites of Ataxin-1 Function

By

Stuart Irwin, B.Sc., MBA

A Thesis

Submitted to the School of Graduate Studies in Partial Fulfillment of

the Requirements For the Degree Master of Science

McMaster University

Master of Science (2004) McMaster University

(Biochemistry) Hamilton Ontario

TITLE: Ataxin-1 Nuclear Bodies are Sub-Nuclear Sites of Function

AUTHOR: Stuart Irwin, B.Sc., M.B.A. (McMaster University)

SUPERVISOR: Dr. Ray Truant

NUMBER OF PAGES: xi, 96

ABSTRACT

Ataxin-1 is the protein affected in Spinocerebellar Ataxia Type 1 (SCA1) polyglutamine neurodegenerative disease. The biological function of ataxin-1 is unknown. By using live cell fluorescence microscopy and cultured human HeLa cells, we have shown that ataxin-1 nuclear inclusions (ataxin-1 NIs) are unique subnuclear sites of ataxin-1 function that do not resemble typical ataxin-1 polyglutamine nuclear aggregates or neuronal intranuclear inclusions (NIIs). Ataxin-1 NIs form independent of polyglutamine expansion in ataxin-1, and we found that ataxin-1 NIs are capable of recruiting the mRNA export factor TAP/NXF1. We propose that ataxin-1 NIs may be more accurately termed ataxin-1 nuclear bodies (ataxin-1 NBs) and suggest that ataxin-1 NBs play a role in mRNA processing and transport. We discovered that the serine to alanine mutation at position 776 of ataxin-1 (S776), known to inhibit spinocerebellar ataxia type 1 (SCA1) pathogenesis, plays a critical role in the frequency and size of ataxin-1 NBs. We found that polyglutamine expansion was not essential for ataxin-1 NB formation, and that serine 776 may be important in turnover regulation of polyglutamine expanded ataxin-1. In addition, we found that serine 776 does not significantly affect nuclear localization of ataxin-1, and that the ataxin-1 associated protein, 14-3-3 zeta, does not have a role in the nucleo-cytoplasmic transport of ataxin-1. These findings reveal that the serine 776-mediated 14-3-3 zeta co-localization with ataxin-1 is likely not important to SCA1 pathogenesis, but that the role of serine phosphorylation of ataxin-1 does have an effect on the formation of ataxin-1 NBs, thereby implicating ataxin-1 NB formation as important for understanding SCA1 disease.

ACKNOWLEDGEMENTS

I would like to thank my supervisor, Dr. Ray Truant, and my committee members past and present, Dr. David Andrews, Dr. Bernardo Trigatti, and Dr. Juliet Daniel for their guidance throughout my graduate studies. I would also like to thank Scott Covey and Christy Thomson for their input, encouragement and support, and Jill Taylor for her appreciation for integrity and conviction for the truth. I would also like to thank Mark VanDelft for his unabashed love of science, Jianrun Xia for his advice and enviably honourable personality, but most importantly for his unreasonably good mood regardless of the day. I would like to thank JoAnne Graczyk for her honesty and naked appreciation for knowledge regardless of whether it was to her benefit or not, Randy Singh for his appreciation for and delivery of objective criticism, Jenny Howell for helping me get started on my project and her honesty about its strengths and weaknesses, and Atooza Rezvampour for her overpowering, excessively emotional but very personal presence in the lab. I will also thank Matt Bates for his honest opinions and stubborn adherence to his beliefs (God bless him), Helen Atkinson for her input on, and supply of a template for, my thesis, as well as the entire Truant Lab for being unwaveringly supportive, helpful, understanding and for dealing just fine with my radical mood swings. I would also like to thank Dr. Gerry Wright and Dr. Denis Daigle for their faith in science, something that is in increasingly short supply in academia. Most importantly I would like to thank everyone in the department who made the Phoenix a fun place to be, even if just for another couple of years.

TABLE OF CONTENTS

LIST OF ABBREVIATIONS

Ataxin-1	The *SCA1* gene product
Ataxin-1 [Q_n]	The *SCA1* gene product with a polyglutamine tract of length n
Ataxin-1 S776A	The *SCA1* gene product with a serine to alanine mutation at position 776
Ataxin-1 wt	The *SCA1* gene product with wild type serine at position 776
$(CAG)_n$	A CAG repeat of length n
DRPLA	Dentatorubropallidoluysian atrophy
eCFP	Enhanced green fluorescent protein (Cyan)
eGFP	Enhanced green fluorescent protein
eYFP	Enhanced green fluorescent protein (Yellow)
FRAP	Fluorescence recovery after photobleaching
GFP	Green fluorescent protein
HD	Huntington's Disease
hnRNP	Heterogenous nuclear RNA binding protein
kDa	KiloDalton
MDa	MegaDalton
mRFP	Monomeric red fluorescent protein
NES	Nuclear export signal
NI	Nuclear inclusion
NII	Neuronal intranuclear inclusion

NLS	Nuclear import signal
NPC	Nuclear pore complex
OD	Optical Density
PBS	Phosphate buffered saline
PCR	Polymerase chain reaction
PML	Promyelocytic leukemia
POMA	Paraneoplastic opsoclonus myoclonus ataxia
Q2	Polyglutamine tract of 2
Q26	Polyglutamine tract of 26
Q84	Polyglutamine tract of 84
Q77	Polyglutamine tract of 77
Q138	Polyglutamine tract of 138
RGB	Red/Green/Blue format
S776A	Serine to alanine mutation at position 776 of ataxin-1
SBMA	Spinal bulbar muscular atrophy
SCA1	Spinocerebellar ataxia type 1
SCA1	The gene that encodes ataxin-1
TIFF	Tagged image file format
TPR	Translocated promoter region

LIST OF FIGURES

INTRODUCTION

1.1 Trinucleotide Repeat Disease

Spinocerebellar ataxia type 1 (SCA1) is one of a growing list of 24 trinucleotide repeat diseases. These diseases are characterized by the expansion of an internal triplet repeat in the causative gene which becomes pathological at about 40 repeats in most cases (Brown *et al.* 2004; Cummings *et al.* 2000; Nakamura *et al.* 2001). This internal DNA repeat can be either in the coding or non-coding region of an affected gene. The most common coding repeat diseases are the $(CAG)_n$ or polyglutamine repeat diseases, as all members of this group have a polyglutamine expansion due to multiple CAG codons inserted into an exon of the gene of interest (Cummings *et al.* 2000). There are six known polyalanine diseases among the coding trinucleotide repeats as well, which are generally pathological at about 15 alanines (Brown *et al.* 2004). The polyglutamine expressing disorders includes Huntington's disease (HD), spinobulbar muscular atrophy (SBMA) (Kennedy's Disease), dentatorubropallidoluysian atrophy (DRPLA), and the spinocerebellar ataxias (SCA1, SCA2, SCA3/Machado-Joseph Disease, SCA6, SCA7 and SCA17) (Cummings *et al.* 2000; Nakamura *et al.* 2001). Interestingly, the polyglutamine diseases are all strictly neurodegenerative, despite ubiquitous expression of the respective protein (Cummings *et al.* 2000), and polyglutamine inclusions are associated with the pathology of each disease (Cummings *et al.* 2000; Huynh *et al.* 2003), although less common in the case of SCA2 (Huynh *et al.* 2003). Progressive neural dysfunction typically begins in mid-life, and is thought to be due to a common mechanism related to the general toxicity of polyglutamine (Cummings *et al.* 2000; Okuda *et al.* 2003). The polyglutamine polar

zipper hypothesis of Max Perutz (Perutz 1994) was proposed as an early explanation of this toxicity. This hypothesis states that the extended polyglutamine tracts are organized into stable aggregates that resist proteolysis. Aggregation of the polyglutamine tracts increase with tract length and this theory supports the notion of a build-up of these aggregates over time (Cummings *et al.* 2000), which is consistent with SCA1 disease.

The instability of trinucleotide repeat DNA is termed "dynamic mutation" and occurs primarily in the CG rich trinucleotide repeats CTG/CAG or CCG/CGG (Richards *et al.* 1992). Faulty replication, recombination and repair mechanisms are all potentially the source of the instability, and the formation of stable secondary and tertiary DNA structures are thought to be the cause (Lenzmeier *et al.* 2003). Although consensus has yet to be achieved on what the actual mechanism of dynamic mutation is, slipped strand intermediates is the favoured hypothesis. A slipped strand intermediate occurs when DNA polymerase stalls on the template during replication and repeatedly replicates a short sequence before it continues, an action called reiterative synthesis (Schlotterer *et al.* 1992). Stable hairpin structures in the DNA resulting in repeat expansion can occur during mitosis or meiosis, reflective of the somatic and germline instability observed in trinucleotide repeat diseases. The formation of a stable hairpin in a DNA Okazaki fragment during replication is thought to produce an expansion. Faulty processing of the 5' flap of the Okazaki fragment during the gap filling step finalizes the error (Lenzmeier *et al.* 2003). This mode of action can also be applied to DNA repair, where gap filling repair could reproduce the conditions of Okazaki fragment ligation (Kovtun *et al.* 2001). CTG/CAG and CCG/CGG repeats are especially prone to the formation of stable hairpins and slipped strand intermediates (Kramer *et al.* 1996; Pearson *et al.* 1996). When DNA

polymerase encounters such a stable secondary structure in the midst of a triplet repeat, reiterative synthesis can occur, expanding the repeat (Schlotterer *et al.* 1992).

1.2 General Characteristics of SCA1 Disease

SCA1 is an autosomal dominant (Orr *et al.* 2001) form of olivopontocerebellar atrophy (Morton *et al.* 1980) with an incidence of approximately one in 100 000. It is caused by the expansion of an unstable trinucleotide repeat in the SCA1 gene that results in a polyglutamine expansion (Banfi *et al.* 1994a; Banfi *et al.* 1994b). It has no cure or effective treatment. Affected individuals display characteristic ataxia, or tremor-like movements early in the disease and their condition slowly degrades until death occurs due to bulbar dysfunction, usually 10-20 years after symptoms first appear (Banfi *et al.* 1994a). Notable epidemiological attributes include genetic anticipation (Banfi *et al.* 1994b) and increased incidence of paternal inheritance (Cummings *et al.* 2000; Orr *et al.* 2001).

1.3 Pathology of SCA1 Disease

Development of SCA1 correlates with a loss of Purkinje cells in the cerebellar cortex (Skinner *et al.* 2001). The cerebellar cortex is responsible for coordination of sensory input and motor control (Johnson *et al.* 2000). Purkinje cells are very large neurons, up to 80 μm in diameter, whose dendritic trees extend from the outer edge of the cerebellum to its centre, making this layer a critical component of the functional area. Purkinje cells receive input from up to 200 000 granule cells each, and provide the only output of the cerebellum, creating the most massive synaptic convergence found in any neuron in the brain (Harvey *et al.* 1991; Johnson *et al.* 2000; Shepherd 1990). Ubiquitin positive neuronal intranuclear inclusions of the

SCA1 gene product, ataxin-1 (ataxin-1 NIIs), (Banfi *et al.* 1994a; Banfi *et al.* 1994b, Koyano *et al.* 2002), are often found in the remaining Purkinje cells of affected individuals. Recent evidence has questioned whether these inclusions are causal factors of SCA1, suggesting that these remaining Purkinje calls are still protected by the presence of inclusions, and Purkinje cells without inclusions were affected first in SCA1 (Watase *et al.* 2002). Degeneration of the inferior olivary nuclei, the cerebellar dentate nuclei, the red nuclei and the nuclei of the third, tenth and twelfth cranial nerves are also observed in many cases, but the Purkinje cells have been the primary focus of research (Orr *et al.* 2001). Pathology is limited to these areas of the brain in both humans and mouse models, despite ubiquitous expression of ataxin-1 throughout the body (Banfi *et al.* 1994b; Orr *et al.* 1993). Ataxin-1 levels vary according to developmental stage and cell type (Banfi *et al.* 1994a), which is characteristic of a highly regulated protein which may act in various cell specific functions.

1.4 The SCA1 Gene Product, Ataxin-1.

Ataxin-1 is an 87 kDa (Banfi *et al.* 1994b; Orr *et al.* 1993) nuclear protein (Klement *et al.* 1998) of unknown function that causes SCA1 disease due to the expansion of an unstable polyglutamine repeat in ataxin-1 encoded by a region of trinucleotide repeats in mutant *SCA1* (Orr *et al.* 2001). This repeat, like all other trinucleotide repeat disorders, displays both somatic and germline instability. This instability increases with length and favours expansion (Cummings *et al.* 2000). Ataxin-1 has recently been shown by J. Howell to participate in nucleocytoplasmic shuttling by fluorescence recovery after photobleaching (FRAP), which suggests it plays a role in both the nucleus and the cytoplasm (Irwin *et al.* in preparation 2004). In keeping with other polyglutamine disorders, the SCA1 phenotype is associated with a

polyglutamine length of 35-40 or more glutamines. The age of onset is proportional to the polyglutamine tract length (Orr *et al.* 2001). Individuals with less than 35 glutamines in both copies of *SCA1* do not develop SCA1, and those with 170 repeats or more in at least one copy develop an early onset form (juvenile) of SCA1. However, whether polyglutamine length affects the rate of disease progression as well, is controversial (Klockgether *et al.* 1998; Orr *et al.* 2001).

Several proteins have been identified to interact with ataxin-1, such as the leucine-rich acidic nuclear protein (LANP, pp32) (Matilla *et al.* 1997; Mutai *et al.* 2000), polyglutamine binding protein (PQBP-1), thought to be involved in polyglutamine toxicity (Okazawa *et al.* 2002), USP7 (a ubiquitin protease) (Hong *et al.* 2002), chaperones, 20s proteasome, AKT kinase, two 14-3-3 isoforms (Chen *et al.* 2003), and p80 coilin, although this is controversial (Hong *et al.* 2003; Skinner *et al.* 1997). Vimentin and actin, as well as some general heat shock proteins, have been identified by immunoprecipitation as interacting with ataxin-1, but these proteins have not been investigated further (Chen *et al.* 2003). None of these interacting proteins have successfully led to elucidation of the normal biological role of ataxin-1. Ataxin-1 has, however, been shown to have RNA binding function *in vitro* that decreases with polyglutamine length (Yue *et al.* 2001). It also contains a nuclear localization signal (NLS) (Klement *et al.* 1998) and a dimerization, or self-association domain (Banfi *et al.* 1996; Chen *et al.* 2003; Cummings *et al.* 2000; Klement *et al.* 1998), which, together with the recent identification of an AXH RNA binding domain provide evidence for a possible role of ataxin-1 in RNA association (Chen *et al.* 2003). This AXH domain is thought to bind RNA with a preference for guanosine and uridine (de Chiara *et al.* 2003), which is consistent with the

findings of Yue *et al.*, in ataxin-1 *in vitro* (Yue *et al.* 2001). The AXH domain is also found in the transcription factor HBP1 (Mushegian *et al.* 1997).

In 1997, Skinner *et al.* (Skinner *et al.* 1997) showed that cultured cells over expressing ataxin-1 form subnuclear structures which were later referred to as ataxin-1 nuclear aggregates (Klement *et al.* 1998), or ataxin-1 nuclear inclusions (ataxin-1 NIs) (Emamian *et al.* 2003). Ataxin-1 NI is the term used to designate these ataxin-1 containing structures observed in cultured cells, while ataxin-1 NII is used to describe aggregated ataxin-1 containing structures in mammalian neurons. Ataxin-1 NIs have been observed frequently in cultured cells overproducing ataxin-1 by transient transfection, but ataxin-1 NIs have not been observed in cultured cells with endogenous levels of ataxin-1 (Skinner *et al.* 1997). It should be noted that no cultured cells have been shown to express ataxin-1 endogenously. Ataxin-1 in ataxin-1 NIs has been shown to be capable of rapid recovery by FRAP (Chai *et al.* 2002; Stenoien *et al.* 2002), and can contain aggregated ataxin-1 (Skinner *et al.* 1997). Ataxin-1 NIs are considered to be analogous to neuronal intranuclear inclusions (NIIs) observed in other polyglutamine diseases (Ross 1997).

1.5 The SCA1 *Transgenic Mouse Model*

In 1995, Burright *et al.*, developed a human ataxin-1 [Q82] transgenic mouse model for studying SCA1 using the Purkinje cell specific promoter pcp2 to focus high level expression on suspected sites of interest in the brain (Burright *et al.* 1995). These mice develop a non-fatal (Watase *et al.* 2002), neurodegenerative condition that causes Purkinje deterioration beginning at approximately eight weeks (Skinner *et al.* 2001), even though mice are not known to develop SCA1 naturally. As SCA1 progresses, dendritic arborisation decreases drastically and the

Purkinje neurons selectively die off, while those that remain contain the signature ataxin-1 NIIs of SCA1 disease (Emamian *et al.* 2003; Skinner *et al.* 2001). At 16-20 weeks, characteristic ataxia is consistently identified by a series of standardized tests of coordination and dexterity (Klement *et al.* 1998; Watase *et al.* 2002). This event coincides with the loss of recognition of ataxin-1 NIIs by an antibody specifically reactive to ataxin-1 phosphorylated at position 776 (Emamian *et al.* 2003) in the remaining Purkinje cells.

The 1996 characterization of a murine *SCA1* gene provided an opportunity to study the effect of a *SCA1* knockout (-/-) in a murine model, an experiment which concluded that the polyglutamine expansion results in a "gain of function" event with respect to ataxin-1 (Matilla *et al.* 1998). Gain of function is attributed to all other polyglutamine diseases as a mode of action (Cummings *et al.* 2000). The SCA1 -/- mouse did not develop ataxia and no other pathology was reported, therefore SCA1 disease is not due to "loss of function". Thus, the reported model of SCA1 disease is that mutant ataxin-1 actively participates in the events that lead to the SCA1 phenotype (Matilla *et al.* 1998). Human polyglutamine expanded *SCA1* has also been knocked into a murine model, and has reportedly resulted in ataxia similar to the transgenic mouse with ataxin-1 expression at normal levels, thus supporting the gain of function mode of action (Watase *et al.* 2002). It is interesting to note that 154 glutamines were used, as 82 were found to be insufficient in this model (Lorenzetti *et al.* 2000). Furthermore, due to the less drastic nature of SCA1 development in this model compared to the transgenic mouse, the human *SCA1* knock-in mouse was used to determine that neurons without NIIs are affected more drastically than those that developed NIIs (Watase *et al.* 2002).

Interestingly, transgenic mouse models incorporating a number of mutations in polyglutamine-expanded ataxin-1 have been reported to reduce or block SCA1 pathology.

Mice with a point mutation that inactivated the nuclear localization signal (NLS) of ataxin-1 did not develop SCA1 disease (Klement *et al.* 1998). A lysine to threonine substitution at position 772 of ataxin-1 [Q77] (Figure 1, Panel A) in a mouse model also did not develop SCA1 and drastically reduced the nuclear localization of ataxin-1 [Q77] (Klement *et al.* 1998). A second mutation, serine to alanine at position 776 (S776A), was found to dramatically reduce SCA1 pathogenesis in mice (Emamian *et al.* 2003). Serine 776 is at the carboxy terminus of the NLS sequence (Figure 1, Panel A). To date, the minimal sequence required for nuclear entry of ataxin-1 is not known, thus, it is unclear whether the NLS of ataxin-1 is affected by the S776A mutation, however, polyglutamine expanded ataxin-1-S776A protein was located in the nuclei in the transgenic ataxin-1 [Q82]-S776A mouse (Emamian *et al.* 2003).

1.6 Post-Translational Modification of Ataxin-1

Serine at position 776 (S776) has been identified as one of two ataxin-1 phosphorylation sites (Emamian *et al.* 2003). Blocking phosphorylation of serine 776 by site directed mutation to alanine has been shown to dramatically reduce the pathogenesis of polyglutamine expanded ataxin-1 in the mouse model, although the mechanism by which this occurs is unknown. The proximity of this residue to the ataxin-1 NLS suggests that serine 776 modification affects nuclear localization (Figure 1, Panel A). This possibility is supported by observations that transgenic mice expressing ataxin-1 [Q82] with either a deleted NLS or an inactivating mutation of the NLS did not develop SCA1 pathology (Klement *et al.* 1998). Other research has suggested that phosphorylation of this residue affects the stability of ataxin-1 as part of a natural turnover cycle (Chen *et al.* 2003). The finding that ataxin-1 in Purkinje cells of ataxin-1 [Q82] transgenic mice is no longer immunoreactive to an antibody specific to

phosphoserine 776 ataxin-1 at 18 weeks (Emamian *et al.* 2003), shortly after the appearance of symptoms consistent with SCA1 development, is of interest as this supports the potential of turnover regulation of ataxin-1 by serine 776.

1.7 The TAP/NXF1 mRNA Export Factor

Pre-mRNAs contain functional splice sites that act functionally as nuclear retention signals, in addition to binding splicing commitment factors. Maturation of pre-mRNA to mRNA involves, among other processing events, the removal of these nuclear retention signals, which allows export of the mRNA product to occur (Chang *et al.* 1989; Legrain *et al.* 1989). Heterogeneous nuclear RNA-binding proteins (hnRNPs) such as hnRNP A1 have been shown to be necessary but not sufficient for nuclear export of mRNA (Lee *et al.* 1996; Nakielny *et al.* 1997), and are bound at a number of sites throughout any single mRNA molecule.

TAP/NXF1, or tip associating protein, has been identified as having a carboxy-terminal sequence responsible for interacting with the nucleoporins in a CRM1 independent export pathway, and later work identified it as the mammalian homologue to the yeast Mex67p protein (Zenklusen *et al.* 2001). Mex67p binds to the hnRNP-like proteins Yra1p and Yra2p in *S. Pombe*, already bound to mRNA (Zenklusen *et al.* 2001). Mex67p acts as the export factor of this complex in an energy dependent manner (Calapez *et al.* 2002) that converges with the CRM1 export pathway at the nuclear pore complex (Schmitt *et al.* 2001). Mex67p acts as a heterodimer with Mtr2 (Santos-Rosa *et al.* 1998), and the complex of these two elements is homologous to the TAP/NXF1 – p15 complex in both structure and function (Fribourg *et al.* 2003; Senay *et al.* 2003). Although it is not currently known whether the TAP/NXF1-p15

complex requires other factors or if it binds directly to mRNA, it has been convincingly shown that TAP/NXF1 is critical for the export of mRNA (Katahira *et al.* 1999; Pasquinelli *et al.* 1997; Saavedra *et al.* 1997). It is thus suspected that TAP/NXF1 binding is the final step before nuclear pore binding and export, since binding of the critical export factor before the splicing events have completed would presumably result in premature export (Cullen 2000).

1.8 14-3-3 Isoforms

Ubiquitously expressed and composing approximately 1% of all soluble protein in the brain, the five 30 kDa 14-3-3 isoforms have recently emerged as a family of extremely important signalling proteins, especially in the nervous system (Fu *et al.* 2000). 14-3-3 was the first signalling molecule identified as a discrete phosphoserine/threonine binding module, and has continued to be of great interest some 36 years after first being discovered (Moore *et al.* 1967). 14-3-3 is found in both the cytoplasm and the nucleus. It can act as a monomer, a homodimer and a heterodimer (Alvarez *et al.* 2003; Takahashi 2003). It is regulated by phosphorylation at as many as three sites (Takahashi 2003), and has been implicated in interactions with ataxin-1 (Chen *et al.* 2003) and over 100 other proteins including vimentin (Takahashi 2003), and HSP1 (Wang *et al.* 2003). It has also been shown to interact with DNA, as cruciform binding protein (CBP) (Alvarez *et al.* 2003). 14-3-3 is also involved in sequestration of several pro-apoptotic members of the Bcl-2 family of proteins (Korsmeyer 1999), and in many cases acts as a bridging protein between two different proteins (Fu *et al.* 2000; Shen *et al.* 2003). Recently, it was found that 14-3-3 zeta (Kousteni *et al.* 1997) and sigma (Leffers *et al.* 1993) interact with ataxin-1 in a manner dependent upon the phosphorylation of serine 776 of ataxin-1 by AKT kinase (Chen *et al.* 2003). This interaction is thought to stabilize

ataxin-1 against degradation and reduce its natural turnover rate, thus contributing to the development of ataxin-1 NIIs (Chen *et al.* 2003). Of further interest is the proximity of this residue to the proposed NLS (Klement *et al.* 1998) (Figure 1, Panel A). It is possible that 14-3-3 binding at this site could result in partial occlusion of the NLS, as 14-3-3 has been shown to participate in phosphorylation dependent molecular interference as a regulatory mechanism in several signalling pathways (Muslin *et al.* 2000). The interaction of 14-3-3 with ataxin-1 involves the zeta and epsilon isoforms, and is dependent upon the specific phosphorylation of ataxin-1 serine 776 (Chen *et al.* 2003). 14-3-3 has been shown to stabilize ataxin-1 against proteolysis and co-localize with ataxin-1 NIs in cultured cells unless serine 776 of ataxin-1 has been mutated to alanine and cannot be phosphorylated (Chen *et al.* 2003). 14-3-3 has a putative nuclear export signal (NES) (Brunet *et al.* 2002; Wurtele *et al.* 2003), which potentially could act to export ataxin-1 to the cytoplasm and contribute to the ability of ataxin-1 to shuttle.

1.9 The Nuclear Pore Complex

In eukaryotic cells, the nucleus is an organelle that is uniquely surrounded by a double lipid membrane, contiguous with the endoplasmic reticulum (ER). Import to and export from the nucleus occurs via the nuclear pore complex (NPC). Small molecules less that 40-60 kDa are able to diffuse through the NPC while larger molecules traverse the pore via an energy dependent translocation process. These larger molecules, whether alone or in a complex with others, must have a signal sequence present that the NPC can recognize, and this signal marks these proteins or complexes for import, export, or both. These sequences, NLS and NES respectively, are peptide sequences than can mediate the nuclear import or export of heterogenous proteins across the NPC. NLSs and NESs are numerous and define different

pathways of nuclear entry and exit. To date, 14 importin family member proteins have been identified. Most factors, aside from importin beta, are involved in RNA and ribosomal protein translocation to and from the nucleus (Moroianu 1997; Weis 2002). Several import and export factors indicate multiple pathways of nuclear transport, each addressed by the cargo protein's import or export signal sequence. A "leucine-rich" NES (Fischer *et al.* 1995), for example, is generally characterized by $LX_{2-3}LX_{2-3}LXL$ (Bogerd *et al.* 1996). The recognition of the leucine-rich NES motif by CRM1 in the presence of RAN-GTP (Fornerod *et al.* 1997) results in the RAN-GTP regulated export of the molecule or complex containing the NES (Fischer *et al.* 1995). A classical importin-dependent NLS can be either mono-partite or bi-partite. A mono partite NLS is loosely characterized as a cluster of basic residues, while its bipartite homologue is characterized by two clusters of basic residues separated by 10-12 residues. The importin heterodimer complex of importins α and β recognize these motifs, binds them and guides them through the NPC into the nucleus, where the import factors are then recycled back to the cytoplasm (Hodel *et al.* 2001).

The NPC is a highly conserved 90-120 MDa tripartite transmembrane complex with eightfold symmetry in the plane of the nuclear membrane (Fahrenkrog *et al.* 2003). There are thousands of NPCs per nucleus, capable of highly selective mass transport on the level of 100 MDa per second each (Keminer *et al.* 1999). It is composed of a nuclear basket and a cytoplasmic ring with eight filaments that reach into the cytoplasm, which are important for recognition of potential transport substrates, and a 90 nm long membrane-spanning pore which is approximately 45-50 nm in diameter (Keminer *et al.* 1999). This diameter coincides with the size of molecules capable of transport, relating physical size to function (Pante *et al.* 2002). Calcium depletion and temperature reduction has been shown to block nuclear

transport reversibly (Bustamante *et al.* 2000; Pante *et al.* 1996; Shahin *et al.* 2001), apparently by allowing the nuclear basket to collapse and trap cargo in transit (Fahrenkrog *et al.* 2003).

Nucleoporin is the name given to the approximately 30 individual components of the NPC (Cronshaw *et al.* 2002). Most of the nucleoporins are found on both the cytoplasmic and nuclear faces of the NPC (Pante *et al.* 1994), but some, such as translocated promoter region (TPR) protein, are only found on the nuclear face (Frosst *et al.* 2002). Gp210/TPR is a 265 kDa component of the nuclear basket, but can be found in nuclear foci in cultured cells (Frosst *et al.* 2002) similar to other nucleoporins, such as Nup98 (Bodoor *et al.* 1999). Some nucleoporins, like Nup98, are found on both nuclear and cytoplasmic faces (Griffis *et al.* 2003) and are thought to shuttle between the nucleus and the cytoplasm along with cargo. Nup98 has been found to preferentially translocate to the cytoplasm when transcription is inhibited (Zolotukhin *et al.* 1999). Nup98 is thought to be responsible for bringing TAP/NXF1 to the nuclear basket for export (Bachi *et al.* 2000; Blevins *et al.* 2003), an interaction which is critical for the export of mRNA from the nucleus. Since the pathology of ataxin-1 in SCA1 disease is clearly affected by nuclear localization of mutant ataxin-1 protein, work in our lab has concentrated on the potential importance and regulation of nucleocytoplasmic transport of ataxin-1 and other polyglutamine disease proteins.

1.10 Experimental Research Approach

The relationship between ataxin-1 NIIs and ataxin-1 NIs observed in cultured cells is unknown. The former is a well characterized protein aggregate associated with SCA1 neuronal pathogenesis (Ross 1997; Skinner *et al.* 1997), while the latter is a structure observed in cultured cells over expressing ataxin-1 (Skinner *et al.* 1997). Ataxin-1 NIs are historically referred to as

polyglutamine aggregates (Cummings *et al.* 1998; Skinner *et al.* 1997), implying that ataxin-1 in nuclear inclusions is misfolded, insoluble, static deposits of protein. However, these inclusions have recently been shown to contain rapidly exchanging components, including proteasomes and chaperones in addition to ataxin-1 (Stenoien *et al.* 2002). We hypothesize that ataxin-1 NIs are not aggregated nuclear protein, but that they are areas of high ataxin-1 concentration likely related to subnuclear sites of ataxin-1 function.

In order to test this hypothesis, we examined ataxin-1 NIs with respect to several characteristics chosen to differentiate them from typical nuclear inclusions or known sub-nuclear structures. First, we tested whether polyglutamine was required for ataxin-1 NIs to develop. Second, the movement of these structures was compared to a fragment of mutant huntingtin protein known to develop *bona fide* nuclear aggregates. Several other proteins are known to form discrete nuclear inclusions or structures. Some of these structures appear similar to ataxin-1 NIs, therefore, we asked, using live cell fluorescence microscopy, if these structures were distinct and separate from other subnuclear structures or whether ataxin-1 NIs are a previously described nuclear sub-structure (Huang *et al.* 1996; Spector 1996). Finally, we tested ataxin-1 NIs for the presence of selected mRNA-associated proteins by live cell fluorescence microscopy.

We have demonstrated that polyglutamine tracts are not necessary for ataxin-1 nuclear inclusion formation. By live cell video fluorescence microscopy, we have found that ataxin-1 NIs are dynamic structures, distinct in location and movement from huntingtin polyglutamine aggregates.

By live cell fluorescence microscopy, we have compared ataxin-1 nuclear inclusion to several known nuclear body-forming proteins to define ataxin-1 inclusions as distinct from

these other known nuclear bodies. We did discover from live cell microscopy that ataxin-1 NIs can recruit the TAP/NXF1 mRNA export factor. Finally, we further characterized the recruitment of TAP/NXF1 by ataxin-1 as being responsive to cellular heat shock.

These results have led to our hypothesis that ataxin-1 nuclear inclusions are not deposits of protein due to polyglutamine expansion and aggregation, but are likely important sites related to the biological function of ataxin-1. Evidence linking ataxin-1 to RNA and the co-localization of TAP/NXF1 in ataxin-1 inclusions implies that ataxin-1's normal biological function may be involved in mRNA processing and/or export.

The modification of serine 776 of ataxin-1 by phosphorylation has been shown to be critical to the development of SCA1 pathology (Chen *et al.* 2003; Emamian *et al.* 2003). Our work in identifying ataxin-1 NIs as sites of ataxin-1 function has brought to our attention the possibility that modification of serine 776 to alanine brings about structural changes in ataxin-1 NIs in addition to specific changes in the stability of ataxin-1. The characterization of changes in these inclusions due to serine 776 modification may be critical to the understanding of SCA1. We hypothesize that the formation of ataxin-1 NIs is affected by phosphorylation of serine 776, and that this modulation by post-translational modification provides an alternate explanation for certain findings in the field of SCA1 research.

In order to test this hypothesis, we conducted experiments to identify differences in the size and number of ataxin-1 NIs. We examined differences due to modification of serine 776 with respect to the distribution and expression of eGFP-ataxin-1 with different polyglutamine lengths, and assessed whether these observed differences were significant. Upon characterization of differences present between wild type and S776A ataxin-1 NIs, we asked whether factoring in these differences would affect the conclusions of co-localization studies

of 14-3-3 zeta with ataxin-1, as colocalization of 14-3-3 with ataxin-1 NIs is currently thought to be directly dependent upon phosphorylation of serine 776 of ataxin-1 (Chen *et al.* 2003).

MATERIALS AND METHODS

2.1 Fluorescence Microscopy

Live cell fluorescence microscopy was conducted with a Nikon TE200 inverted fluorescence microscope with a 175W zenon arc lamp (Sutter Instruments LB-LS/17), using Nikon 100x or 60x plan apochromat oil immersion objectives (numerical apertures 1.3 and 1.40, respectively) where indicated. Filter sets (Chroma) denoting bandpass excitation and emission filters for each fluorescent protein or dye used are as follows. mRFP: set 31004; excitation D560/50x, emission D630/60m. dsRED: set 31002; excitation D540/25x, emission D605/55m. eYFP: set 31040; excitation D480/30x, emission D535/40m. eGFP: set 41017; excitation D470/40x, emission D525/50x. eCFP: set 31044v2; excitation D436/20x, emission D480/40m, Hoechst dye: set 31000; excitation D360/40x, emission D460/50m. Images were collected using a monochrome camera, which captured images in each channel separately (Hamamatsu model C4742-95 and controller). Control of the instruments, merging and pseudocolouring of the unbinned images was done using Simple PCI version 5.2.0.2404 (Compix) software. Digital deconvolution was performed using Autodeblur version 9.1 (Autoquant Imaging, Inc.) Gold Edition. Corel Photopaint version 11 (Corel Corporation) was used to sharpen and adjust brightness and contrast for some images for publication.

2.2 Laser Confocal Microscopy

Laser confocal fluorescence micrographs were captured on a Carl Zeiss LSM 510 Laser Scanning Microscope (Zeiss) using 488 nm 200 mW argon (Lasos, LGK 7802) and 543

nm five mW helium-neon (Lasos LGK 7786) lasers for excitation and a 63X water objective (numerical aperture 1.2) (McMaster Imaging Facility) with proprietary software (Zeiss Instruments LSM 510 Scanning Control Program, version 2.3) at a resolution of 1024 x 1024 pixels. Control of the instruments, merging and pseudocolouring of the images was done using this proprietary software. Emission filters used for each fluorescent protein used are as follows. MRFP: LP 560 with a secondary dichroic FT 545 beam splitter (Zeiss LSM 510 standard) at position NFT1. eGFP: BP 505-530 (Zeiss LSM 510 standard).

2.3 Co-Localization Studies

Cultured human HeLa cells (American Tissue and Cell Collection, ATCC, CCL-2) were used for all co-localizations. Cells were transfected with appropriate amounts of the identified constructs and protein expression was analyzed over an 8-36 hour period to adjust for the idiosyncratic expression and fluorescence profiles of the constructs used. The minimum expression time possible for clear images was chosen for each study in order to reduce the possibility of artefacts due to over expression. At the conclusion of expression, cells were imaged using either laser confocal microscopy or fluorescence microscopy, as specified. Co-localizations were identified by qualitative assessment of fluorescence micrographs. Fluorescent signatures of separate fluorescent fusion proteins with increased local concentrations in identical positions seen consistently over the majority of images captured is the working definition of co-localization for the purposes of this manuscript, and is digitally defined by a third pseudocolour in merged images.

2.4 Expression Plasmids

MRFP-C1 was made by JoAnne Graczyk using mRFP cDNA (Campbell *et al.* 2002) (kind gift, Roger Tsien, Department of Pharmacology, University of California at San Diego). The mRFP insert was amplified by PCR using primers RT0335 and RT0337, cut with Nhe1 and BspE1 restriction endonucleases and ligated into eGFP-C1 using T4 DNA ligase. eGFP-C1 was cut with BspE1 and Nhe1 restriction endonucleases.

All constructs containing ataxin-1 were made by cloning into the Multiple cloning site (MCS) of eCFP-C1 (BD Clonetech), eGFP-C1 (BD Clonetech), eYFP-C1 (BD Clonetech) or mRFP-C1 (as described above) using EcoRI and Xba1 restriction endonucleases and subsequent ligation with T4 DNA ligase. eGFP-ataxin-1 [Q26] and eGFP-ataxin-1 [Q84] were created from the original constructs amplified by PCR using mutagenic 5' and 3' primers RT0313 and RT0314 which added EcoRI and Xba1 restriction endonuclease sites respectively, from eGFP*-ataxin-1 [Q26] and eGFP*-ataxin-1 [Q84] (kind gift, HT Orr, University of Minnesota, MN) and were subsequently cloned into eGFP-CI. eGFP-ataxin-1 [Q2] was created from eGFP*-ataxin-1 [Q26] by Mark VanDelft using reverse PCR with primers to the polyglutamine repeat, RT0323 and RT0324, incorporating only a single glutamine at each end and blunt-end ligated using T4 DNA ligase. eGFP-ataxin-1 [Q2] was used to create eCFP-ataxin-1, eYFP-ataxin-1 and mRFP-ataxin-1. Ataxin-1 [Q84] S776A (kind gift, HT Orr, Institute of Human Genetics, University of Minnesota, MN) was amplified by PCR using RT0313 and RT0314 and it was cloned into eGFP-C1. It was subsequently cloned into the eCFP-C1 MCS using EcoRI and XbaI restriction endonucleases and a subsequent ligation with T4 DNA ligase. eGFP-ataxin-1 [Q26] S776A and eGFP[Q2] S776A were constructed from eGFP-ataxin-1 [Q84] S776A using BamHI and Xba1 restriction endonucleases to remove the

3' sequence, which was then ligated into eGFP-ataxin-1 [Q26] with T4 DNA ligase and eGFP-ataxin-1 [Q2]. Ataxin-1 [Q26] K772T was constructed using a recombinant PCR method (Ho *et al.* 1989; Horton *et al.* 1989). The internal mutation of lysine to threonine made use of complementary mutagenic primers RT0527 and RT0528 with 5' and 3' primers RT0494 and RT0314. This fragment was cut with BamHI and Xba1 restriction endonucleases, and ligated into eGFP-ataxin-1 [Q26] using T4 DNA ligase at the complementary sites. eYFP-ASF and mRFP-ASF were constructed from eGFP-ASF (kind gift, D Spector, Cold Spring Harbour) using PstI and HinDIII restriction endonucleases a nd subsequent ligation with T4 DNA ligase into eYFP-C1 and mRFP-C1. eCFP-TAP/NXF1 (JoAnne Grakzyk), eGPF-TAP/NXF1 (JoAnne Grakzyk), eYFP-TAP/NXF1 (JoAnne Grakzyk) and TAP/NXF1-mRFP were constructed from TAP/NXF1 (kind gift, Brian Cullen, Howard Hughes Medical Institute and Department of Genetics, Duke University Medical Center, Durham, NC) through amplification by PCR using mutagenic 5' and 3' primers, RT0329 and RT0330, which added BamHI and EcoRI sites respectively. This fragment was digested with BamHI and EcoRI restriction endonucleases and subsequently ligated with T4 DNA ligase into each of eCFP-C1, eGFP-C1 eYFP-C1 and mRFP-C1. mRFP-14-3-3 zeta was constructed from 14-3-3 zeta pcDNA3.1 (kind gift, H Zoghbi, Baylor College of Medicine, Houston, TX). 14-3-3 zeta was amplified by PCR using mutagenic 5' and 3' primers, RT0422 and RT0424, which added EcoRI and Xba1 restriction endonuclease sites respectively, digested with EcoRI and Xba1 restriction endonucleases and ligated into mRFP-C1 with T4 DNA ligase. mRFP-14-3-3 zeta was digested with EcoRI and Xba1 restriction endonucleases to supply a 14-3-3 zeta insert for eCFP-C1 and eYGP-C1 to create eCFP-14-3-3 zeta and eYFP-14-3-3 zeta, ligation was completed using T4 DNA ligase. mRFP-14-3-3 [NESI] zeta was created using mRFP-14-3-3

zeta as a template for site-directed mutagenesis by a recombinant PCR method (Ho *et al.* 1989; Horton *et al.* 1989). Complementary primers incorporating a point mutation, RT0430 and RT0431, for a leucine to serine 227 substitution were used with the original 5' and 3' primers for EcoRI and Xba1 used in the construction of the template. The 14-3-3 [NES1] zeta product was ligated into the mRFP-C1 MCS using EcoRI and Xba1. The identical procedure was used to construct mRFP-14-3-3 [NESII] zeta, using mRFP-14-3-3 [NESI] zeta as a template with primers RT0472 and RT0473, targeting a second leucine to serine substitution at position number 225 (Figure 1, Panel B). eGFP-Nup98 (kind gift, M Powers, Emory University School of Medicine, Atlanta, GA), eGFP-PML (kind gift, Sato Lab, National Institute of Infectious Disease, Tokyo, Japan), eGFP-gp210/TPR (kind gift, L Gerace Lab, The Scripps Research Institute, La Jolla, CA) and pCaspase3-Sensor (BD Clonetech) were also used.

All enzymes used for DNA cloning were supplied by New England Biolabs or Fermentas Biotech.

2.5 Tissue Culture

All data was collected from transiently transfected human HeLa epithelial carcinoma cells (American Tissue and Cell Collection, ATCC, CCL-2) grown in Gibco Dulbecco's Modified Eagle Medium (Invitrogen Corporation) with 10% Gibco Fetal Bovine Serum - Qualified (Invitrogen Corporation) at 37°C and 10% CO_2.

Cells were grown to 80% confluence and passaged using Trypsin-EDTA (Invitrogen Corporation). A hemocytometer was used to count cells and to ensure that 25 mm glass bottomed dishes were seeded with approximately 70 000 - 140 000 cells 48 hours before

transfection. Glass bottomed 25 mm culture dishes were prepared using a slightly modified, previously described procedure (Howell *et al.* 2002).

2.6 Transfections

Glass bottomed 25 mm culture dishes were prepared using a slightly modified previously described procedure (Howell *et al.* 2002). 18mm circular coverslips were used to reduce uneven seals and dishes were rinsed with cold sterile PBS instead of allowing them to air-dry. These dishes were used for all transfections unless otherwise specified. All transfections were carried out using polyethylimine (Exgen 500, Fermentas) and the protocol supplied by Fermentas (Fermentas Retrieved Jan 2004). All transfections involving ataxin-1 moieties in any vector, eGFP-PML, eGFP-gp210/TPR, eGFP-Nup98, ASF/SF2 in all forms and pCaspase3-Sensor (BD Clonetech) used oneμg of DNA unless otherwise specified. mRFP-14-3-3 zeta was transfected using 0.5 μg of DNA in every case. mRFP-TAP/NXF1 was transfected using 1.5 μg of DNA and eYFP-TAP/NXF1 was transfected using only one μg. Reporter plasmids mRFP and eGFP were transfected using only 0.5 μg of DNA in every case. Quality of DNA was measured, where stated, by OD 260/280 (Biophotometer RS232 C, Eppendorf).

2.7 Hoechst Staining of Live Cells

Cells in 25 mm culture dishes were incubated for one hour in the presence of 75 ?g/μl Hoechst dye (#33342, Sigma-Aldrich), followed by two washes of room temperature PBS and reconstitution with media.

2.8 eGFP-ataxin-1 Moieties and Quantitation

Number of inclusions, size of inclusions, total fluorescence and average percent nuclear localization measurements were collected from the same cells which were allowed to express eGFP-ataxin-1 for 12 hours. Cells that expressed for only eight hours were used only for average percent nuclear localization and total fluorescence due to underdevelopment of inclusions at this short expression time. Fluorescent plasmid constructs were expressed in *E.Coli*, purified and quantitated using OD 280 at exactly the same time in order to reduce differences introduced by storage conditions. These constructs were then diluted to 500 ng/ul, quantitated an additional three times and averaged in order to obtain an accurate measurement. Samples with individual measurements deviating 5% or more from the mean were rejected and the sample was measured an additional three times. OD260/280 ratios were used as relative measures of DNA purity and were also measured three times and subjected to the same control. Samples with average ratios outside of the arbitrarily designated 1.80-1.86 window were rejected and the preparation of the plasmids was repeated until adequate purity of all constructs was achieved at the same time. HeLa cells from the same passage were split into four separate dishes and grown to 80-90% confluence. Each dish was used to seed three, 25 mm glass-bottomed dishes to 140 000 cells as precisely as possible. These cells were transfected exactly four hours later with one μg of eGFP-ataxin-1 and 0.5 μg of mRFP and centrifuged (Beckman Coulter Allegra 6 with GH 3.8 rotor) for one minute at 400 RPM using swinging buckets (Beckman Microplus carrier) with custom made plexiglass stabilizers that hold three, 25 mm tissue culture dishes each. Exactly seven or 11 hours later they were treated

with Hoechst dye resulting in a final time of eight or 12 hours. Fluorescence microscopic imaging followed immediately for no more than 20 minutes per dish.

After random selection of cells (Self Blinded Selection, Appendix A), each cell was micrographed twice using the 60X objective with an unbinned capture resolution of 256x256 pixels, once with a 50 ms exposure in the eGFP channel for standardized measurement of fluorescence (set 1), and once with the eGFP exposure adjusted so that the images were of similar maximum brightness (set 2), using the histogram provided with image by Simple PCI. Images in the Hoechst and mRFP channels were unchanged between micrographs. This adjusted image was used to collect data on the ataxin-1 nuclear inclusions. Each image was contrast and brightness adjusted in both the red and blue channels so that the entire cell was represented by an intensity of 255 in the red channel, and the nucleus was represented by an intensity of 255 in the blue channel. The green channel was not adjusted in this procedure. These images were all saved as 24 bit RGB TIFF (tagged image file format) files for quantitation.

Adjusted 24 bit images were imported into Simple PCI as a single data document. Total cellular fluorescence, roundness, area, maximum intensity and minimum intensity were collected using the motion tracking analysis capabilities of Simple PCI. The "Identify" settings were as follows. Red: minimum (255), maximum (255). Blue and green channels were left unconstrained. The "modify" application was used for single passes of "full prune" and "fill holes". A minimum area of 500 μm^2 only using the "qualify" menu filtered out small pieces of other cells and small imaging artefacts. During data collection, problem cells were flagged for possible exclusion. A problem cell was defined as one whose nucleus was incompletely stained with Hoechst dye, or that was obviously dead. A second pass of data collection was required

for nuclear fluorescence. The "identify" menu was altered to select for areas with both red and blue intensities of 255, and the "qualify" menu was altered to select for only objects with a minimum area of 100 μm^2. The "runtime" menu allowed for Hoechst dye artefacts to be removed during data collection by adjusting exclusion criteria where needed. A third pass using set two was required in order to collect the data on the ataxin-1 nuclear inclusions. Identification requirements were red (255), blue (255) and green (100-255). The attribute "separate" was used only in this pass in order to separate nearly merged inclusions, and qualification required a minimum inclusion size of 100 nm^2. All three datasets were aligned so that each attribute measured was associated with a single record and saved.

2.9 Statistical Analysis

SPSS version 11.5 software (SPSS Inc.) was used to produce all graphs and statistical analyses. Independent samples T-tests were used to determine significance. In order to adjust significance for conducting multiple tests, the Bonferroni correction (Sankoh *et al.* 1997) was used to determine an appropriate p-value to determine significance of differences using the equation $\alpha^1=\alpha^\circ/N$ where α° is the standard score by which a p-value indicates significance (0.05 used here), N is the number of tests conducted and α^1 represents the new score required to determine significance. For the determination of significance of the number and sizes of ataxin-1 NIs, 0.006 was used as α^1 since all of the effects of polyglutamine moieties and serine 776 mutants were compared to each other, resulting in eight comparisons (Figure 7, Panel E, F). In the case of total fluorescence and average percent nuclear fluorescence, all four moieties were compared to each other, polyglutamine and serine 776 mutants were compared as single

groups, as well as comparisons across both expression systems making 36 comparisons and an α^1 of 0.0014 (Figure 7, Panels G, H).

2.10 Heat Shock of TAP/NXF1 and Ataxin-1 Nuclear Inclusions

Cells were co-transfected with 1.5 μg of mRPF-TAP/NXF1 and 0.5 μg eGFP-ataxin-1 [Q26 or Q84] in Delta T 0.18mm 1.5 ml heated tissue culture dishes (Bioptechs Inc.), and the subsequent expression of the fusion proteins took place over approximately 24 hours to ensure a strong fluorescent signal from mRFP-TAP/NXF1. Suitable cells were identified by having well developed ataxin-1 nuclear inclusions, good general morphology and no visible recruitment of mRFP-TAP/NXF1 signal into the existing ataxin-1 nuclear inclusions. Selected cells were imaged at T=0 minutes. The temperature was immediately raised to 42°C for five minutes and another micrograph was taken. At this point, the heat was turned off completely and the culture dish was allowed to cool to ambient temperature for 25 minutes, with micrographs being taken at five-minute intervals. At T=30 minutes, the temperature was rapidly raised to 37°C and imaging continued every five minutes to T=60 minutes. Throughout this time, CO_2 levels were approximately maintained by manually adjusting the heated lid (Bioptechs Inc.), which contained a CO_2 port fed by a Vera Verastaltic Pump Plus (Manostat) with a flow speed of four.

Chapter 1: Ataxin-1 Nuclear Inclusions are Subnuclear Sites of Function

RESULTS CHAPTER ONE

3.1 Ataxin-1 Nuclear Inclusions are Dynamic Bodies Distinct From Huntingtin Nuclear Inclusions

Several polyglutamine disease proteins including ataxin-1 are seen to form intranuclear neuronal inclusions (Ross 1997), or ataxin-1 NIIs. A well-described example is huntingtin protein (DiFiglia *et al.* 1997). The presence of aggregated huntingtin in the nucleus is highly correlated with Huntington's disease, a characteristic shared by SCA1 with ataxin-1 NIIs. To address potential similarities between ataxin-1 NIs and huntingtin nuclear aggregates, we designed experiments to observe these inclusions in live cells by the use of GFP (Green Fluorescent Protein) fusion technology. In our experiments, we used an enhanced variant of GFP, eGFP or SG5T, which fluoresces 35x brighter than wild type V. aquaria GFP protein (Cormack *et al.* 1996). We expressed eGFP-ataxin-1 [Q84] in HeLa cells by transient transfection and visually detected dynamics of ataxin-1 inclusions at 37°C. We qualitatively compared the movement of ataxin-1 nuclear inclusions to those of eGFP-huntingtin exon1 [Q138] protein (Xia *et al.* 2003) (Figure 2). Time course images were taken at identical two frame per second frame rates for 30 seconds (Figure 2, Panels A,B), and three-dimensional voxel images were generated using time in the Z plane (Figure 2, Panels C,D). The voxel images were then thresholded to the relatively high fluorescence intensity of the inclusions only for both ataxin-1 and huntingtin protein (Figure 2, Panels E,F). By comparing movement

of individual inclusions of ataxin-1 and huntingtin protein (Figure 2, Panels G, H), we could see that ataxin-1 inclusions could translate 1-2 μm, whereas huntingtin inclusions, either cytoplasmic or nuclear, remained static.

To determine if nuclear inclusion formation and other observed properties of ataxin-1 protein were polyglutamine dependent, we used inverse PCR to remove all but two polyglutamine residues from human ataxin-1 protein. As seen in figure 3, the formation of nuclear inclusions of ataxin-1 was not dependant on the presence of polyglutamine. Ataxin-1 [Q2] also displayed similar inclusion dynamics to ataxin-1 [Q26] or [Q84] (Supplemental Videos 3-5). From this data, we observed that ataxin-1 inclusion formation was polyglutamine independent and that ataxin-1 nuclear inclusion dynamics were different from huntingtin polyglutamine aggregates.

3.2 Ataxin-1 Inclusions Recruit a Messenger RNA Export Factor

It has been shown by fixed cell immunofluorescence that ataxin-1 did not co-localize with the coilin coiled body component, p80, the spliceosome component, SC35, and the transcription factor, Bcl-6 (Skinner *et al.* 1997). Furthermore, ataxin-1 re-distributed promyelocytic leukemia (PML) protein (Skinner *et al.* 1997). These studies were extended to examine the nuclear speckle protein, ASF/SF2 (Misteli *et al.* 1997). In human HeLa cells expressing eCFP-ataxin-1 and eYFP-ASF/SF2, no co-localization was observed. In fact, eYFP-ASF/SF2 appeared to be excluded from areas occupied by ataxin-1 NIs (Figure 4A Panels A-C). In addition, no co-localization was seen between eGFP-ataxin-1 and the dsRED fusion of the pre mRNA/mRNA binding protein, hnRNPA1 (Siomi *et al.* 1995) (Figure 4A Panels D-F). However, co-localization was observed between eGFP-ataxin-1 [Q2] and

mRFP-TAP/NXF1 protein, a mRNA export factor (Segref *et al.* 1997) in live cells, at ataxin-1 inclusions (Figure 4A Panels G-I). No colocalization was observed between eGFP-gp210/TPR protein (Bodoor *et al.* 1999), a nuclear structural protein (Figure 3 B, Panels A-C), eGFP-huntingtin exon-1 [Q138] (Figure 4B, Panels D-F) or nup98, a dynamic nuclear pore complex protein observed to form nuclear inclusions (Bodoor *et al.* 1999) (Figure 4B Panels G-I). Therefore, despite the RNA binding ability and RNA-dependant localization of ataxin-1, eGFP-ataxin-1 did not localize with splicing or mRNA processing factors. In live cells, eGFP-ataxin-1 was not seen to co-localize or re-distribute promyelocytic leukemia (PML) bodies (Figure 4B, Panels J-L). In this experiment, only mRFP-TAP-NXF1 was found to co-localize with ataxin-1 NIs.

The connection between ataxin-1 and TAP/NXF1 was also seen with polyglutamine-expanded ataxin-1 (Figure 5, Panels A-D). TAP/NXF1 was not recruited to eGFP-labelled huntingtin exon-1 [Q138] inclusions in live cells, even when over-expressed (Figure 5, Panels E-H). When expressed alone in live cells, TAP/NXF1 localized entirely to the nucleus, but remained evenly distributed in the nucleoplasm, exclusive of nucleoli, with no inclusion formation (Figure 5, Panels M-O) (Irwin *et al.* in preparation 2004). Therefore, it appeared that TAP/NXF1 protein could be specifically recruited to ataxin-1 nuclear inclusions.

While we could see endogenous TAP/NXF1 co-localizing with ataxin-1 in all fixed cells (Figure 5, I-L) observed by immunofluorescence (image by Ray Truant for Irwin *et al.* in preparation 2004), the degree of co-localization of mRFP-Tap/NXF1 with eGFP-ataxin-1 in live cells (Figure 4A, Panels G-I, Figure 5, Panels E-H), was variable. The co-localization in live cells appeared to be enhanced when the cells were subjected to heat or cold-shock (i.e. cooling on ice prior to fixation). We then asked whether the cellular stress of heat shock would

affect the recruitment of Tap/NXF1 to ataxin-1 inclusions (Figure 6). Human HeLa cells, co-transfected with mRFP-TAP/NXF1 and eGFP-ataxin-1, were heat shocked at 42°C for five min and then observed by two-channel fluorescence microscopy at 37°C at ten-minute intervals for one hour. As seen in Figure 6, heat-shock caused the progressive recruitment of mRFP-TAP protein to eGFP-ataxin-1 NIs (Figure 6, Panels C-H). In contrast, mRFP protein alone co-expressed with ataxin-1 did not co-localize to ataxin-1 NIs in one hour after heat shock (Panels K-M), nor did mRFP-TAP/NXF1 localize to nuclear structures after heat shock in the absence of ataxin-1 (data not shown).

DISCUSSION CHAPTER ONE

4.1 The Ataxin-1 Cell Culture Model

The biological function of ataxin-1 is not known. Ataxin-1 nuclear inclusions (ataxin-1 NIs) have yet to be observed as an endogenous structure in cultured cells, but form readily when ataxin-1 is highly expressed and have been linked to the presence of aggregated ataxin-1 (Matilla *et al.* 1997; Skinner *et al.* 1997). It is important to note, however, that endogenous ataxin-1 is not known to be expressed in any cultured cell line. High expression alone, however, is not responsible for the formation of these structures (Skinner *et al.* 1997). Ataxin-1 neuronal intranuclear inclusions (ataxin-1 NIIs) found in SCA1 diseased Purkinje cells are described as ubiquitin positive ataxin-1 aggregates similar to those observed in Huntington's disease. Ataxin-1 NIIs are thought to develop due to a polyglutamine expansion in the SCA1 gene product, ataxin-1, and are not thought to occur naturally in healthy Purkinje cells (Klement *et al.* 1998; Vig *et al.* 2000). Ataxin-1 NIs in cultured cells are thought to be analogous to ataxin-1 NIIs, and cultured cell models are used here to demonstrate selected properties of ataxin-1. Using green fluorescent protein (GFP) technology in these studies had advantages over alternative technologies. First, a single fluorophor per molecule allowed quantitation of the relative amount of the protein of interest present. Second, 100% fluorescent signal specificity cannot be achieved by immunofluorescence, but could by using a fluorescent protein fusion, assuming negligible proteolytic cleavage. In the case of ataxin-1, an amino-terminal fusion of a fluorescent protein appears to form identical structures to carboxy-terminal FLAG-tagged (Klement *et al.* 1998) or internally FLAG-tagged ataxin-1 (Skinner *et al.*

1997), and the use of live cell fluorescent microscopy eliminates the possibility of artefacts due to the fixation process, as well as a new, living cell observation system for ataxin-1.

4.2 Relevance of the Normal Biological Function of Ataxin-1

Understanding of ataxin-1 function is critical to the development of potential therapy for spinocerebellar ataxia type 1 (SCA1), as has been recently demonstrated with the androgen receptor, responsible for spinal bulbar muscular atrophy (SBMA). It was determined for SBMA that a polyglutamine expansion in a cell surface androgen receptor was the source of polyglutamine aggregates found in the nuclei of affected neurons in SBMA-affected individuals. Research concluded that testosterone binding resulted in the activation of a signal transduction pathway that imported the ligand bound androgen receptor to the nucleus where, in the case of polyglutamine expansion, the receptor formed the protein aggregates thought to be responsible for SBMA. This data suggested that if the androgen receptor were to be prevented from entering the nucleus, disease could be averted. Recently, researchers have found that chemical blockers that deplete testosterone, the androgen receptor ligand, reduced nuclear import of the androgen receptor, and have been found to be an effective treatment for SBMA, actually reversing both the behavioural and histopathological phenotype (Katsuno *et al.* 2003). Thus, the success of developing a therapy for this disease depended directly upon the fact that the normal biological function of the androgen receptor was well known. This example highlights the need to establish the biological function of ataxin-1 in order to design a disease-specific therapy for SCA1. More importantly, it shows that polyglutamine diseases, while all caused by polyglutamine expansion, may all be treatable by completely unrelated therapies related to the biological function of their respective proteins.

4.3 Ataxin-1 Nuclear Inclusions are Distinct Dynamic Bodies

Our data shows that ataxin-1 NIs that result from expression of fluorescent labelled ataxin-1 differ from polyglutamine nuclear aggregates formed by polyglutamine expanded huntingtin exon-1 [Q138]. While huntingtin exon-1 [Q138] nuclear aggregates reportedly form due to the polyglutamine expansion present in eGFP-huntingtin exon-1 [Q138], ataxin-1 NIs can form in the absence of polyglutamine. Furthermore, co-expression of both eCFP-ataxin-1 [Q2] and eGFP-huntingtin exon-1 [Q138] resulted in the formation of distinct intranuclear structures. While this does not prove that ataxin-1 NIs are not aggregated protein, it does suggest that they occur due to the inherent characteristics of ataxin-1, other than polyglutamine expansion. Furthermore, the weak mobility of inclusions formed by huntingtin exon-1 [Q138] compared to ataxin-1 NIs, and the roundness along with the unique localization throughout the nucleus of ataxin-1 NIs compared to huntingtin aggregates, suggests that ataxin-1 NIs are not immobile protein aggregates similar to huntingtin aggregates. Further evidence of this has been provided by others using fluorescence recovery after photobleaching (FRAP) (Chai *et al.* 2002; Stenoien *et al.* 2002). The eGFP-ataxin-1 present in ataxin-1 NIs was able to move rapidly within the nucleus, presumably as soluble protein. Also demonstrated was the ability of ataxin-1 to shuttle to and from the nucleus, (not shown) implying that either ataxin-1 has an unidentified nuclear export signal (NES), or it is exported by another protein or complex that does (Irwin *et al.* in preparation 2004). Therefore, ataxin-1 NIs are unlikely to be immobile random protein aggregates, and do not form solely due to polyglutamine expansion.

The implication that ataxin-1 NIs are not random aggregates suggests some degree of organization is responsible for their occurrence. Ataxin-1 NIs look like both promyelocytic leukemia (PML) bodies and interchromatin granule clusters, or nuclear speckles. Nuclear speckles were described by David Spector of Cold Spring Harbour in 1992 (Huang *et al.* 1992) as being subnuclear domains harbouring mRNA processing machinery. Ataxin-1 has been found previously to bind RNA *in vitro* and contain an RNA binding motif (Chen *et al.* 2003; de Chiara *et al.* 2003; Yue *et al.* 2001). Therefore, the possibility of an interaction with nuclear speckles would have suggested a role for ataxin-1 in mRNA processing. Our finding that ataxin-1 is not found at elevated levels in areas occupied by nuclear speckles shows that ataxin-1 NIs are not nuclear speckles, and the qualitative observation that ataxin-1 NIs appear to actually create areas of lower concentration of ASF/SF2 suggests that there is either active reorganization by ataxin-1 NIs that excludes other proteins, or that ataxin-1 and ASF/SF2 are competing for similar factors.

PML bodies are subnuclear structures similar to nuclear speckles, and are similar to ataxin-1 NIs. They have been implicated in post-translational modification and storage of subnuclear factors, control of apoptosis, viral pathogenicity and are even thought by some to be random nuclear aggregates (Eskiw *et al.* 2003; Grande *et al.* 1996; Regad *et al.* 2001). Endogenous PML, a component of PML bodies, has been shown to be present in structures similar yet distinct from ataxin-1 NIs (Skinner *et al.* 1997). This experiment, however, compared highly over expressed FLAG-tagged human ataxin-1 to an endogenous PML protein at endogenous levels in COS cells. The possibility exists that ataxin-1 NIs, due to massively over expressed ataxin-1 in this context, artefactually re-distributed protein, and since the cells were fixed in this experiment, the result is not necessarily the behaviour of either

protein in living cells. We have taken three steps to avoid over expression artefacts with ataxin-1 expression; firstly, we used HeLa cells, a human cell line that does not replicate transfected plasmids; secondly, we did not exceed 1-2 μg of DNA per transfection in a 25 mm dish; and finally, most observations were done within 18-24 hours of transfection, a fraction of the time used by others, often 72 hours in plasmid-replicating COS cells. In these COS cells, published images show a single ataxin-1 inclusion that encompasses most of the nucleus (Chen *et al.* 2003). We did not observe this level of expression throughout any of the work presented here.

PML bodies have been found to assume different conformations, making comparison with a single endogenous species a further concern. Live cell fluorescence microscopy has shown that PML bodies exhibit a motion (Muratani *et al.* 2002) very similar to that of ataxin-1 NIs (Figure 2, Panel H). This information has prompted us to re-examine PML bodies as possible sites of ataxin-1 function. We found that even as over expressed eGFP variant fusions in human cells, PML and ataxin-1 formed separate and distinct subnuclear structures (Figure 4B, Panels J-L). GFP variant proteins have been used where possible in the place of more red shifted fluorescent proteins when comparing nuclear structures in order to reduce the influence of structurally different fusions. Ataxin-1 NIs were compared in the same manner to gp210/TPR (Byrd *et al.* 1994) and Nup98 nuclear inclusions (Bachi *et al.* 2000; Radu *et al.* 1995), both of which form nuclear inclusions similar to ataxin-1 in cultured cells. gp210/TPR is thought to be a nucleoporin, localized to the nucleoplasmic face of the nuclear pore (Frosst *et al.* 2002), as is Nup98, which is thought to directly interact with TAP/NXF1 (Blevins *et al.* 2003) at the nuclear pore. The finding that ataxin-1 NIs differ from these structures is further evidence that ataxin-1 NIs have a distinct identity and are not formed due to polyglutamine aggregation or properties of over expression of GFP variant fusions proteins. This data is

supportive of our tissue culture and transient transfection model to research ataxin-1 biological function.

Ataxin-1 NIs appear to have a distinct identity, thus, it is reasonable to assume that ataxin-1 NIs may also have a distinct function. The occurrence of ataxin-1 NIs in the presence of increased ataxin-1 expression levels, which are known to fluctuate drastically during somatic and neural development (Banfi *et al.* 1996; Banfi *et al.* 1994a; Orr *et al.* 1993), suggests that the formation of ataxin-1 NIs is very likely related to ataxin-1 function. Identification of other factors present in ataxin-1 NIs are then of great use in elucidating ataxin-1 function. Based on the ability of ataxin-1 to shuttle between the nucleus and cytoplasm and to bind RNA, along with accumulated evidence that the nucleus is the primary subcellular site of mutant ataxin-1 induced pathogenesis, we chose to follow this line of research into the function of ataxin-1 NIs within the nucleus. To this end, we investigated the possible roles of ASF, hnRNP A1 and TAP/NXF1 in ataxin-1 NIs.

Co-localization studies with ataxin-1 and hnRNP A1, a protein generally associated at multiple sites with pre-mRNA and mRNA from transcription through processing and export, showed that hnRNP A1 was not found at increased local concentrations in ataxin-1 NIs. TAP/NXF1, however, was found to co-localize with ataxin-1 NIs in some cells, and further investigation found that this could be increased to all cells once subjected to heat shock. This is potential evidence of regulation at the level of ataxin-1 NIs, specifically with respect to a global, mandatory export factor for mRNA. It is possible that, since TAP association is suspected of being the final step before mRNA export (Cullen 2000), ataxin-1 NIs are the site of this final export signal activation for a specific group of mRNA transcripts delivered by ataxin-1. One such transcript appears to have been identified as GluRI (Private

Communication, HT Orr, Institute of Human Genetics, University of Minnesota, MN), which codes for a subunit of the AMPA receptor, a glutamate receptor (Zamanillo *et al.* 1999). This suggests that ataxin-1 may play a role in maintenance of cell-cell signalling, possibly explaining the high sensitivity of Purkinje cells to ataxin-1 mutation. Potentially, the stress induced by heat shock results in a regulatory response designed to facilitate expression of these mRNA transcripts, making these transcripts the key to elucidation of the role of ataxin-1. Since TAP/NXF1 is a universal mRNA export factor, the effect of ataxin-1 is likely not at the protein level, but possibly at the level of any specific RNA species bound by ataxin-1. We propose, based on the evidence presented here regarding the characteristics of ataxin-1 NIs, we could more accurately refer to ataxin-1 NIs as ataxin-1 nuclear bodies.

4.4 Possible Roles of Ataxin-1

The question of what the biological role of ataxin-1 is remains. Evidence regarding RNA metabolism is accumulating with respect to the development of SCA1 disease. Disruption of mRNA processing or transport has precedence in neurological disease. Fragile X syndrome, another of the triplet repeat diseases, results from mutation of the gene product of the *FMR1* gene, FMRP (Eberhart *et al.* 1996). A CGG expansion in the 5' untranslated region results in a loss of function in FMRP which, in turn reduces the export of important mRNA transcripts for brain development (Fridell *et al.* 1996). The result is down regulation of these important mRNAs and the development of mental retardation in Fragile X affected individuals (Brown *et al.* 2001; Kaytor *et al.* 2001). NXF5 is a putative RNA export factor and is absent in some patients with X-linked mental retardation (Jun *et al.* 2001). SMN1 interacts with hnRNP R and Q, and is expressed at reduced levels in the brains of patients affected by spinal

muscular atrophy (Rossoll *et al.* 2002). hnRNPs are associated with mRNA throughout pre-mRNA processing and maturation (Cullen 2000). Recently, NOVA proteins have been identified as specific pre-mRNA splicing antigens in the autoimmune disorder, paraneoplastic opsoclonus myoclonus ataxia (POMA). These proteins regulate the splicing of specific neuronal pre-mRNA transcripts, three quarters of which code for proteins which function at the neuronal synapse. The regulatory dysfunction of the expression of these synaptic proteins results in a form of ataxia (Ule *et al.* 2003).

Ataxin-1 may be comparable in function to SR proteins, a group of factors involved in pre-mRNA processing (Blencowe *et al.* 1999). Nuclear speckles, the structure primarily associated with ASF/SF2, are thought to be storage areas for specific SR proteins (Blencowe *et al.* 1999), and this may also be true for ataxin-1 nuclear bodies. While we did not see ataxin-1 co-localized to nuclear speckles, we did note the exclusion and re-distibution of eYFP-ASF/SF2 away from ataxin-1 nuclear bodies, which raises the possibility of competitive interactions. SRm160, a splicing co-activator, interacts specifically with certain SR proteins (Longman *et al.* 2001) and shares an area of loose homology with ataxin-1 that covers the NLS of ataxin-1. While this homology is less than 50%, the sequence homology occurs with a periodicity of six residues, and may be indicative of a shared interaction domain. Continuing ataxin-1 research will be directed at SR proteins as a potential model for ataxin-1 biological function.

Chapter 2: Serine 776 of Ataxin-1 Affects Ataxin-1 Nuclear Bodies

RESULTS CHAPTER TWO

5.1 Serine 776 of Ataxin-1 Affects Ataxin-1 Nuclear Bodies

Here, we analyze data from a set of experiments designed to identify the immediate effects of serine 776 modification on the formation of ataxin-1 nuclear bodies. We considered changes in size and number of ataxin-1 nuclear bodies, changes in total cellular eGFP-ataxin-1 content and eGFP-ataxin-1 nuclear localization of transfected cells, and finally, changes in co-localization of eGFP-ataxin-1 with previously described proteins.

By live cell analysis, we confirmed qualitative observations (Figure 7, Panels A-D) that mutation of serine 776 to alanine (S776A) resulted in the formation of ataxin-1 nuclear bodies that were smaller ($p<0.006$) (Figure 7, Panel E) and more numerous ($p<0.006$) (Figure 7, Panel F) in cultured human HeLa cells in the case of both eGFP-ataxin-1 [Q26] and eGFP-ataxin-1 [Q84]. The number and size of ataxin-1 nuclear bodies was not significantly different between eGFP-ataxin-1 [Q26] and eGFP-ataxin-1 [Q84] ($p=0.966$ and $p=0.673$).

5.2 Serine 776 of Ataxin-1 Affects Ataxin-1 Inclusion Formation

We compared total fluorescence of four different eGFP-ataxin-1 moieties ([Q26] wt, [Q26] S776A, [Q84] wt, [Q84] S776A) in transfected cultured Human HeLa cells between eight and 12 hour expression systems. We found significant differences in total fluorescent protein content (Figure 7, Panel G), explained in detail below.

At eight hours post-transfection, eGFP-ataxin-1 [Q84] average total fluorescence levels were lower than eGFP-ataxin-1 [Q26] levels, and this difference was found to be significant ($p<0.0014$). There was no significant difference between the fluorescence of wild type and S776A mutants within these groups ([Q26] $p=0.325$; [Q84] $p=0.736$). At 12 hours post-transfection, however, the ataxin-1 [Q26] average total fluorescence levels had failed to register a significant increase ($p=0.984$) while ataxin-1 [Q84] fluorescence levels had risen, and were now in fact higher than ataxin-1 [Q26] fluorescence levels, both observations being significant ($p<0.0014$). Furthermore, within the 12-hour expression eGFP-ataxin-1 [Q84] moieties, the average total fluorescence level of ataxin-1 [Q84] S776A was found to be significantly higher than ataxin-1 [Q84] wt, while this is not true for the eGFP-ataxin-1 [Q26] moieties of the same expression time ($p=0.754$). This suggests that eGFP-ataxin-1 [Q84] S776A was more stable to proteolysis than its wild type eGFP-ataxin-1 [Q84] wt counterpart.

After establishing that moiety dependent differences exist in the overall expressed levels of ataxin-1, we asked whether polyglutamine expansion or modification of serine 776 had an effect upon the nuclear localization of ataxin-1 (Figure 7, Panel H). After eight hours of expression in HeLa cells, ataxin-1 [Q84] was found to be significantly more nuclear than ataxin-1 [Q26] ($p<0.0014$). Interestingly, ataxin-1 S776A was not found to be significantly more nuclear than its wild type counterpart ($p=0.0015$), although its very low pvalue is considered as potentially important. After 12 hours of expression, the relationship between polyglutamine and nuclear localization was reversed, as seen previously with respect to total fluorescence. The average percent nuclear fluorescence of eGFP-ataxin-1 [Q26] was found to be significantly greater than that of eGFP-ataxin-1 [Q84] ($p<0.0014$). Conversely, the average

measured fluorescence of eGFP-ataxin-1 S776A was found to be significantly higher than that of eGFP-ataxin-1 wt ($p<0.0014$), unlike in the 8-hour expression system.

The differences between eight and 12 hour expression systems were also investigated. The increase in eGFP-ataxin-1 [Q26] and the decrease in eGFP-ataxin-1 [Q84] percentage nuclear fluorescence when expressed for an additional four hours were both found to be significant ($p<0.0014$), while no significant difference was found between the measured average percent nuclear fluorescence of either eGFP-ataxin-1 wt or eGFP-ataxin-1 S776A between the eight and 12 hour expression systems (eGFP-ataxin-1 wt $p=0.383$; eGFP-ataxin-1 S776A $p=0.101$).

5.3 14-3-3 zeta Does Not Export Ataxin-1 from the Nucleus

Considering that differences have been established between ataxin-1 nuclear bodies according to ataxin-1 moiety, we asked whether co-localizations of other proteins with ataxin-1 nuclear bodies were affected as well. MRFP tagged 14-3-3 zeta co-localized with ataxin-1 nuclear bodies regardless of polyglutamine expansion (Figure 8, Panels G-K). Mutation of serine 776 did not block co-localization of mRFP-tagged TAP/NXF1 with ataxin-1 nuclear bodies (Figure 8, Panels L-Q), which suggests that the actual protein content of ataxin-1 nuclear bodies is not affected by S776A mutation. We further found that, while others have found moiety dependent co-localization of 14-3-3 zeta with ataxin-1 nuclear bodies (Chen *et al.* 2003), when ataxin-1 nuclear bodies of similar size were compared, co-localization of mRFP-14-3-3 zeta was maintained (Figure 8, Panels R-Z). In order to test the specificity of mRFP-14-3-3 interaction with ataxin-1 nuclear bodies, we asked whether mRFP-14-3-3 zeta also co-localized with other subnuclear structures and with eGFP-huntingtin exon-1 [Q138]

aggregates. We found that mRFP-14-3-3 zeta co-localized with all subnuclear structures investigated (Figure 9, Panels A-L), but did not co-localize with the aggregated protein of huntingtin exon-1 [Q138] (Figure 9, Panels M-O), nor with eGFP alone (Figure 9, P-R). This potentially non-specific co-localization of mRFP-14-3-3 zeta with nuclear structures lead us to test the effect of nuclear localization of ataxin-1 on 14-3-3 localization to ataxin-1 nuclear bodies. We found that mRFP-14-3-3 co-localized with ataxin-1 structures in both the nucleus and cytoplasm when the NLS and putative 14-3-3 binding site was altered mutating lysine 772 to threonine (Figure 1, Panel A, Figure 10, Panels E-H), not observed with an mRFP control (Figure 10, Panels A-D). This mutation has been previously found to reduce ataxin-1 transport to the nucleus (Klement *et al.* 1998), and falls within the 14-3-3 binding site proposed by Chen *et al.* (Chen *et al.* 2003). We further tested the specificity of mRFP-14-3-3 zeta interaction with ataxin-1 by mutating the proposed active site and/or putative NES of 14-3-3 (Rittinger *et al.* 1999; Zilliacus *et al.* 2001). Leucines 245 and 247 were mutated to serines (Figure 1B), and no loss of co-localization with ataxin-1 nuclear bodies was observed (Figure 11, Panels D-I). Of further interest was the lack of obvious change in the overall nuclear localization of mRFP-14-3-3 zeta NES mutants, now lacking the consensus NES required for CRM1 dependent export.

The presence of 14-3-3 zeta in the nucleus of seemingly healthy cells may not be due to import by ataxin-1, so we asked whether 14-3-3 zeta was imported into the nucleus during its participation in signal transduction pathways of apoptosis (Masters *et al.* 2002). To test this, we investigated the relationship between caspase 3 activation and nuclear localization of mRFP-14-3-3 zeta. Caspase3 Sensor is a cytoplasmic construct that is imported into the nucleus upon activation of caspase 3, a step in apoptosis. This plasmid expresses a caspase cleavage site between three NLSs and an NES, as an eYFP fusion, such that when the reporter

protein is cleaved, the NES is removed and the protein localizes primarily to the nucleus. Our studies showed that nuclear localization of 14-3-3 did not correlate completely to caspase 3 activation as indicated by Caspase3 Sensor (Figure 12, Panels C-H), thus we concluded that 14-3-3 nuclear localization was not the result of caspase 3 mediated cell apoptosis.

DISCUSSION CHAPTER TWO

6.1 Mutation of Serine 776 of Ataxin-1 Affects the Morphology of Ataxin-1 Nuclear Bodies

Recent evidence has shown that serine 776 of polyglutamine-expanded ataxin-1 is critical to the development of SCA1 in transgenic mice (Emamian *et al.* 2003). It is also a known site of phosphoregulation through AKT kinase (Chen *et al.* 2003), however the link between these two findings and pathogenesis is unknown. Our cell model has shown that ataxin-1 nuclear bodies appear to be sites of localization related to ataxin-1 function. Insight into the function of ataxin-1 may provide therapeutic options to light for patients with SCA1 disease, and indicate potential methods to delay the onset of symptoms in individuals genetically pre-disposed to developing SCA1. In the case of ataxin-1, we have used a cellular model to demonstrate that serine 776 of ataxin-1 may be crucial to the function and regulation of ataxin-1, by testing the effect of serine 776 to alanine mutation on the properties of ataxin-1 nuclear bodies and ataxin-1 distribution.

In cells expressing mutant ataxin-1 S776A, ataxin-1 nuclear bodies are significantly smaller and more numerous than those expressing ataxin-1 with wild type S776. The size of the polyglutamine tract did not have a significant impact on the number or size of ataxin-1 nuclear bodies in our constructs of 26 and 84 glutamines, considered in both S776A and wild type contexts. Ataxin-1 nuclear bodies have been shown to be unique nuclear structures (Irwin *et al.* in preparation 2004), and we have found that serine 776 has a significantly greater impact on the morphology of ataxin-1 nuclear bodies than pathological polyglutamine expansion. From this, we conclude that serine 776 of ataxin-1 plays an important role in natural function

of ataxin-1, likely due to phosphoregulation by AKT kinase noted by Chen *et al.*, (Chen *et al.* 2003) or another kinase. This finding further supports our previous observations that polyglutamine expansion is not responsible for ataxin-1 nuclear body formation, and suggests that we have identified phosphorylation of ataxin-1 as affecting properties of ataxin-1 nuclear bodies. The fact that a single point mutation in ataxin-1 could have a significant impact in inclusion formation leads us to believe that these ataxin bodies are not likely due to protein over-expression, but are instead regulated sites of high local concentration of ataxin-1.

6.2 Mutation of Serine 776 of Ataxin-1 Affects Ataxin-1 Levels in a Cellular Model

By comparing the expression levels of ataxin-1 over time and across four moieties, we have found that polyglutamine expansion and mutation of serine 776 can influence each other to alter total ataxin-1 levels on our model system. eGFP-ataxin-1 [Q26] expression levels of both wt and S776A moieties remained essentially steady between our eight and 12 hour observations, suggesting that the proteolytic degradation of ataxin-1 in this context was roughly equal to its production during this time. Conversely, eGFP-ataxin-1 [Q84] wt and S776A moieties were a lower level in the first eight hours of expression, suggesting that either they were expressed at a slower rate, which is unlikely because all moieties employ the same promoter, or that they were experiencing more effective degradation. Investigation of trinucleotide repeats has shown that the formation of stable hairpins in extended CAG/CTG repeat DNA affects replication; these effects may slow transcription and/or translation of the affected protein. No data has been shown to suggest that this occurs in polyglutamine disease, and polyglutamine inclusions do not repress transcription in general, although polyglutamine proteins do (Hoshino *et al.* 2004), making this scenario plausible. It is also possible that

constitutive expression of the larger polyglutamine expanded ataxin-1 may take more time or cellular resources, explaining lower ataxin-1 levels of polyglutamine-expanded ataxin-1 at eight hours, although polyglutamine expanded ataxin-1 is only six percent larger than unexpanded ataxin-1.

Alternatively, polyglutamine expanded ataxin-1 [Q84] may be more specifically targeted for proteolysis than polyglutamine unexpanded ataxin-1 [Q26]. After an additional four hours of expression time, we found that not only had eGFP-ataxin-1 [Q84] levels increased significantly, eGFP-ataxin-1 [Q84] had increased to a level significantly greater than eGFP-ataxin-1 [Q26]. This observation suggests that proteolysis of polyglutamine expanded ataxin-1 is inhibited, a finding consistent with others (Chen *et al.* 2003). This data suggests that the observation of polyglutamine expanded ataxin-1 at levels lower than polyglutamine unexpanded ataxin-1 at eight hours may be more easily explained by inhibition of expression than by more effective targeting by proteolytic machinery, and the subsequent relative increase in ataxin-1 levels supports a conclusion of inhibition of degradation due to polyglutamine expansion.

Finally, eGFP-ataxin-1 [Q84] S776A appears to be at levels greater than eGFP-ataxin-1 [Q84] wt after 12 hours of expression, a finding that is inconsistent with Chen *et al.* (Chen *et al.* 2003). Chen *et al.,* found that serine 776 of ataxin-1 in COS cells over expressing 14-3-3 zeta was responsible for the stabilization of ataxin-1. Our findings suggest that in the absence of over expressed 14-3-3 zeta, in a human cell model system, increased stability of ataxin-1 [Q84] S776A may occur due to the inability of alanine 776 to be phosphorylated. We propose that serine 776 of ataxin-1 plays a role in regulation of the turnover of ataxin-1. The Purkinje cells of transgenic ataxin-1 [Q82] mice are no longer immunoreactive to an antibody specific to

phosphorylated ataxin-1 at 18 weeks, a time when ataxin-1 NIIs are prevalent. Dephosphorylation of ataxin-1 may inactivate it, or have another regulatory effect meant to decrease its effect in the cell. Our observation of increased stability may indicate shortcomings of our model since these are not neural cells, but that fact that this point mutant has an effect remains important. In addition, it has been noted that ataxin-1 NIIs do not contain 14-3-3 (Private Communication from HT Orr, Institute of Human Genetics, University of Minnesota, MN), suggesting that the ataxin-1 in ataxin-1 NIIs is not phosphorylated, and that ataxin-1 NIIs may not be sites of function, and that they are not ataxin-1 NIs. This data is further evidence that phosphorylation of serine at position 776 (S776) is involved in regulation of ataxin-1 levels in the context of expanded polyglutamine, and our evidence shows that there may be an interaction effect between polyglutamine expansion and the ability of position 776 to regulate ataxin-1 levels.

We also asked whether modification of serine 776 affected the function of the NLS of ataxin-1. We found that, over time, eGFP-ataxin-1 [Q26] became more localized to the nucleus. Since ataxin-1 nuclear bodies form in the first 48 hours after transfection, it is possible that as the ataxin-1 nuclear bodies develop, they recruit ataxin-1 more effectively. This would explain the increase in nuclear localization of eGFP-ataxin-1 [Q26]. It is also possible that ataxin-1 nuclear export requires certain limited factors that are at insufficient levels to move ataxin-1 into the cytoplasm when ataxin-1 levels have increased after 12 hours of expression. We also found that polyglutamine expanded eGFP-ataxin-1 [Q84] was more nuclear than eGFP-ataxin-1 [Q26] moieties after eight hours, suggesting that nuclear export was inhibited in eGFP-ataxin-1 [Q84] moieties, as compared to eGFP-ataxin-1 [Q26] moieties. Finally, our finding that eGFP-ataxin-1 [Q84] becomes less nuclear over time is not easily

explained until expression levels are considered. eGFP-ataxin-1 [Q26] levels remained steady over time, while becoming more nuclear, suggesting that independent of total levels, polyglutamine unexpanded ataxin-1 accumulates in the nucleus. eGFP-ataxin-1 [Q84], found at lower levels than eGFP-ataxin-1 [Q26] after eight hours of expression, is more nuclear. Over the subsequent four hours, eGFP-ataxin-1 [Q84] becomes significantly less nuclear and significantly more abundant. This finding suggests that expression levels of ataxin-1 in this model do affect nuclear localization, an effect that may confound our attempts to quantify the effect of polyglutamine expansion and serine 776 modification on the cellular distribution of ataxin-1. The earlier suggestion that proteolysis may affect different moieties with differing effectiveness also raises the question of the effect of proteolytic cleavage of the eGFP tags from ataxin-1, as proteolytic cleavage could result in a misleading distribution of the fluorescent signal.

We did not find a significant effect of serine 776 modification on the cellular distribution of eGFP-ataxin-1, suggesting that phosphorylation of ataxin-1 does not affect nuclear localization as was previously thought. Three different mutations of the NLS of polyglutamine expanded ataxin-1 in transgenic mouse models were non pathogenic: complete deletion, K772T and S776A, with S776A appearing completely nuclear. Our work has shown that a serine to alanine mutation at position 776 (S776A) does not alter nuclear localization, indicating that ataxin-1 [Q82] transgenic mice with this particular mutation averted SCA1 symptoms for a different reason that it was averted in the case of the NLS disrupted mutants. Drawing this distinction is an important step toward gaining a deeper understanding of the molecular pathology of ataxin-1. Our data further suggests that the polyglutamine expansion of ataxin-1 [Q84] has an effect on the stability of ataxin-1 that is exaggerated in the presence of

S776A. However, the lack of nuclear localization effect with ataxin-1 S776A may also reveal a limitation of our cell culture model, as there are likely some important differences between our tissue culture cells and human primary neurons, or transgenic Purkinje cells from mice.

6.3 14-3-3 zeta is Present in Ataxin-1 Nuclear Bodies Independent of Ataxin-1 Serine 776 Modification

It has been shown by others that 30 kDa maltose binding protein (MBP), amino-terminal fusion to 14-3-3 do not block dimerization or substrate binding (Alvarez *et al.* 2003), so we do not forsee any difficulties with our 26 kDa fluorescent protein fusions. We used an mRFP fusions to the amino-terminus of 14-3-3 zeta, and were initially able to reproduce previously reported findings that 14-3-3 zeta co-localized with only wild type serine 776 ataxin-1 and not alanine 776 mutants. However, upon establishing certain differences in properties of ataxin-1 nuclear bodies of various moieties, we became concerned with the possibility of misinterpretation of our data by altered ataxin-1 nuclear body properties, not altered ataxin-1 properties. Other researchers have found that smaller ataxin-1 nuclear bodies are less prone to co-localization with factors such as ubiquitin than larger ataxin-1 nuclear bodies (Stenoien *et al.* 2002). Once we controlled for this by selecting ataxin-1 nuclear bodies of a size and frequency similar to ataxin-1 wt, we found that ataxin-1 S776A nuclear bodies did co-localize with mRFP-14-3-3 zeta. As was shown with polyubiquitin by Stenoien et al., (Stenoien *et al.* 2002), the smaller ataxin-1 NIs did not appear to co-localize with mRFP-14-3-3 zeta, and it is possible that these smaller ataxin-1 NIs are inactive, as seen with ataxin-1 NIIs observed to be dephosphorylated in SCA1 murine Purkinje cells at 18 weeks (Emamian *et al.* 2003). We further found that mRFP-14-3-3 zeta was recruited into PML bodies, Nup98 nuclear foci,

gp210/TPR nuclear foci, SCA1 NIs and even with cytoplasmic ataxin-1 nuclear bodies resulting from eGFP-ataxin-1 [26] K772T NLS mutant (Figure 1, Panel A). The finding that mRFP-14-3-3 zeta did not co-localize with eGFP-exon-1 [Q138], the only known structure of aggregated protein of those we tested, suggests that perhaps there is a degree of specificity to the interaction of mRFP-14-3-3 zeta with subnuclear sites of function, as opposed to the colocalization of mRFP-14-3-3 zeta being an artefact of over expression of eGFP-labelled protein structures. These findings suggest only that 14-3-3 is present in ataxin-1 nuclear bodies for reasons not related to serine 776 of ataxin-1, perhaps as a bridging molecule, a common role for 14-3-3 dimers (Fu *et al.* 2000). Therefore, while 14-3-3 may bind to all nuclear bodies tested, including ataxin-1, the factors bridged and composition of 14-3-3 heterodimers may be different (Alvarez *et al.* 2003).

6.4 14-3-3 zeta Does Not Affect the Nuclear Localization of Ataxin-1

In order for a protein or complex of proteins to shuttle, it must be capable of import to and export from the nucleus, and we considered each action separately for 14-3-3 and ataxin-1. First, we hypothesized that 14-3-3 was present in the nucleus of our ataxin-1 model cell system because it was imported through the nuclear pore complex (NPC) bound to ataxin-1, and used the NLS of ataxin-1 for import. Second, we hypothesized that ataxin-1 was exported to the cytoplasm through the NPC bound to 14-3-3 zeta, and the putative NES of 14-3-3 was responsible for export by the CRM1 dependent pathway. We and others have shown that 14-3-3 zeta is found in ataxin-1 nuclear bodies, even though 14-3-3 zeta does not have a putative NLS, and we do not observe consistent and obvious nuclear bodies in the absence of ataxin-1. Our second hypothesis, that ataxin-1 was exported from the nucleus by

14-3-3 zeta lead us to mutate the nuclear export signal (NES) of mRFP-14-3-3 zeta by changing two critical leucine residues to serines (Figure 1, Panel B). Leucine residues 225 and 227 are identified as highly conserved across species and isoforms of 14-3-3 (Rittinger *et al.* 1999), and are required by the leucine-rich NES consensus (Bogerd *et al.* 1996). These residues are further implicated as important residues for ligand binding, for example with p53 or CRM1 (Liu *et al.* 1995; Petosa *et al.* 1998; Rittinger *et al.* 1999; Wurtele *et al.* 2003). We did not observe an increase in the nuclear content of mRFP-14-3-3 zeta [NESII] when alone or when co-expressed with ataxin-1. Our observations of mutant mRFP-14-3-3 [NESII] zeta did not differ in any way from our observations of wild type mRFP-14-3-3 zeta. These findings indicate that the putative NES of 14-3-3 zeta does not provide the export signal for ataxin-1.

We made an inactivating mutation in the NLS of eGFP-ataxin-1 [Q26] K772T (Figure 1, Panel A) as per Klement *et al.*, (Klement *et al.* 1998) in order to determine whether reducing the ability of ataxin-1 to localize to the nucleus would affect the nuclear mRFP-14-3-3 zeta content, our first hypothesis. We found that mRFP-14-3-3 zeta could still be present in the nucleus, even though this mutation virtually eliminated ataxin-1 nuclear localization and formation of ataxin-1 nuclear inclusions, although cytoplasmic ataxin-1 containing structures were observed. This finding indicates that 14-3-3 zeta is not imported into the nucleus by ataxin-1 alone.

We also showed that the presence of mRFP-14-3-3 in the nucleus is not due to caspase 3 mediated apoptosis. In cells expressing mRFP-14-3-3, there is a great deal of variability with respect to the nucleocytoplasmic distribution of our mRFP-14-3-3. Since our data explains neither the presence of 14-3-3 in the nucleus nor the fluctuation in its nuclear levels, we considered the possibility that the cells that appeared to have greater amounts of

mRFP-14-3-3 in the nucleus were actually in different stages of apoptosis. Our data shows that cells that appear apoptotic according to the function of commercial Caspase3 Sensor do not consistently have increased mRFP-14-3-3 zeta in the nucleus. The data in this study suggests that mRFP-14-3-3 zeta is present in the nucleus and ataxin-1 nuclear bodies for reasons other than import or export with ataxin-1, or apoptosis.

6.5 Concluding Remarks

The tendency to aggregate, resistance to proteolysis, structural changes affecting function, interaction with polyglutamine specific factors in the cell, these are all potential factors in the development of a polyglutamine disease, and it is likely that every one of them has an effect on every polyglutamine disease to some extent. Toxicity may occur when the total contribution of these factors and the biological context of the affected protein results in pathology, and this may not depend completely on any one effect. Polyglutamine expansion can potentially cause aggregation, disrupt or enhance protein interactions, inhibit transport, and sequester cofactors, all in the same disease. For this reason, we must consider all observations of changes induced by polyglutamine expansion in ataxin-1 as contributing to SCA1.

The polyglutamine diseases are neurodegenerative. Historically, polyglutamine neuronal intranuclear inclusions were thought to be the cause of neurodegeneration, but recently, researchers have cast doubt on this direct relationship, suggesting that polyglutamine inclusions are a common symptom of these diseases and not necessarily toxic themselves (Hoshino *et al.* 2004). In the case of SCA1, aggregated ataxin-1 seen in the neuronal nuclei of diseased SCA1 brains may be related to dysfunction and aggregation of ataxin-1 nuclear

bodies. Our work here has shown that ataxin-1 nuclear bodies form even in the absence of polyglutamine tracts, move in what appears to be an energy dependent manner and react to heat shock induced cell stress by recruiting TAP/NXF1, a general mRNA export factor. We suggest that ataxin-1 nuclear bodies participate in the processing and export of a specific group of mRNAs, and dysfunction of ataxin-1 may affect the ability of ataxin-1 nuclear bodies to function effectively, leading to aggregation of ataxin-1 at these areas of increased ataxin-1 concentration. This could be the nucleation event of an ataxin-1 NII from a dysfunctional and perhaps unseen ataxin-1 NI in nature. As shown with SR proteins in nuclear speckles (Blencowe *et al.* 1999), ataxin-1 nuclear inclusions may be areas of protein sequestration of ataxin-1 or staging areas for ataxin-1 association with pre-mRNAs or mRNAs prior to export.

We have shown that modification of a critical phosphoregulated serine residue can affect properties of ataxin-1 nuclear bodies, directly linking pathogeneic mechanism of ataxin-1 to the structure of ataxin-1 nuclear bodies. The recruitment of TAP/NXF1 into ataxin-1 nuclear bodies in response to heat shock is important to this theory, as mRNA association with TAP/NXF1 is thought to be the last step required before export of mRNA to the cytoplasm, and response to cellular stress may reveal the nature of the transcripts of mRNAs thought to be exported. Signal starvation has been implicated as the cause of Purkinje cell death in SCA7 (Garden *et al.* 2002), and together with the identification of a glutamate receptor mRNA transcript, GluRI, as a possible ataxin-1 ligand, perhaps SCA1 pathology follows a similar pathway. Furthermore, since we have eliminated 14-3-3 as the export factor for ataxin-1, TAP/NXF1 could be a candidate export factor for ataxin-1, further implicating an mRNA connection to SCA1 pathogenesis. The visible formation of ataxin-1 nuclear bodies in tissue culture may be due to the overproduction and/or reduced turnover of ataxin-1 aggravated by

lack of specific mRNA transcripts required to fulfill a cytoplasmic function of ataxin-1 that would move ataxin-1 out of the nucleus. Excess ataxin-1 in ataxin-1 nuclear bodies may aggregate over time and inhibit the natural function of ataxin-1, and this would be accelerated by polyglutamine expansion of ataxin-1. In SCA7, two separate populations of NIIs have been identified, one giving rise to the other over time as proteins accumulate in SCA7 NIs (Takahashi *et al.* 2002), which is also observed in ataxin-1 nuclear bodies (Stenoien *et al.* 2002). We propose that ataxin-1 binds a specific family of mRNA transcripts, and that ataxin-1 is active at least partly in the cytoplasm. Ataxin-1 may localize mRNA to a specific cytoplasmic area, perhaps via vimentin or actin that was identified in recent immunoprecipitation of ataxin-1 (Chen *et al.* 2003). Recent data from our lab has shown that ataxin-1 cytoplasmic inclusions, sometimes seen in transfected HeLa cells, are significantly more frequent in a neuronal cell line (Private Communication from J. Graczyk, Department of Biochemistry, McMaster University), expected to have more mRNA transcripts related to the AMPA gluamate receptor. The role of 14-3-3 and phosphorylation of serine at position 776 in this pathway is unclear, and it is in this area that further important work must be done before the role of ataxin-1 in the brain is understood. As for potential therapies and targeted drug design against SCA1 for the distant future, mouse model data clearly indicates that specific exclusion of ataxin-1 from the nucleus, or the specific inhibition of the ataxin-1 phosphorylation of serine at position 776 of ataxin-1 are valid drug targets. Elucidation of the specific roles they play in SCA1 pathogenesis will impact the design of these potential therapies.

FIGURES

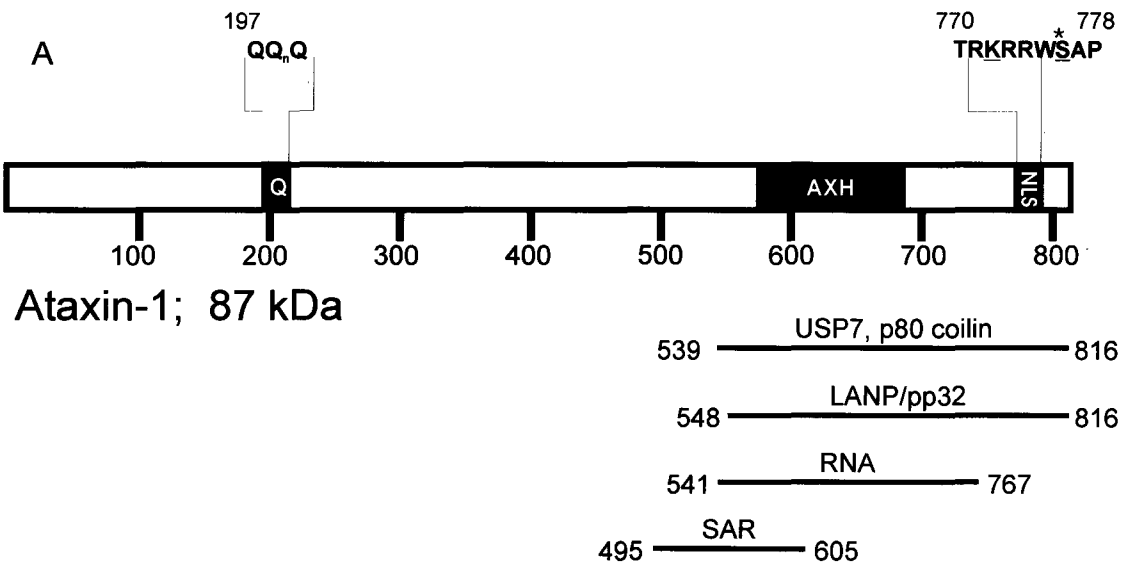
A
197
QQnQ
770
778
TRKRRWSAP
Q
AXH
NLS
100
200
300
400
500
600
700
800
Ataxin-1; 87 kDa
USP7, p80 coilin
539
816
LANP/pp32
548
816
RNA
541
767
SAR
495
605

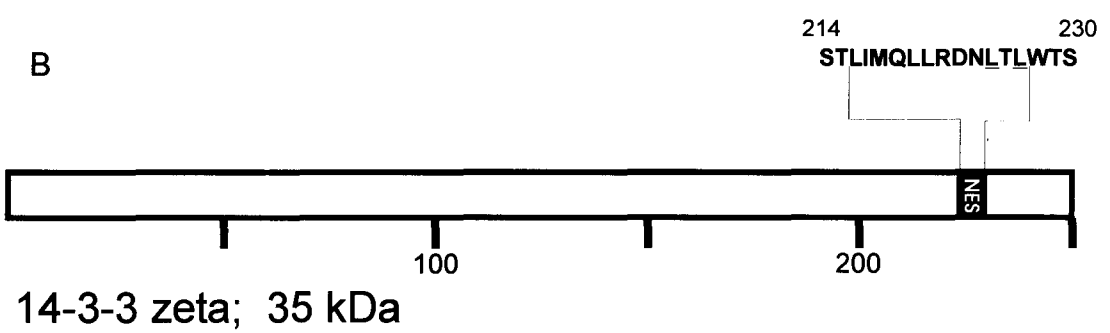
B
214
230
STLIMQLLRDNLTLWTS
NES
100
200
14-3-3 zeta; 35 kDa

Figure 1

Figure 1. Ataxin-1 and 14-3-3 zeta Maps with Relevant Features. Residues that have been modified in the preceding experiments are underlined. Panel A, Ataxin-1 with polyglutamine tract (Q), AXH domain (AXH), nuclear localization signal (NLS), self-association region (SAR), RNA binding domain (RNA), LANP/pp32 binding domain (LANP/pp32) and proposed binding domain for USP7 and p80 coilin. Serine 776 is indicated with *. Reproduced from de Chiara et al., 2003 (de Chiara *et al.* 2003). Panel B, 14-3-3 zeta with NES indicated by NES.

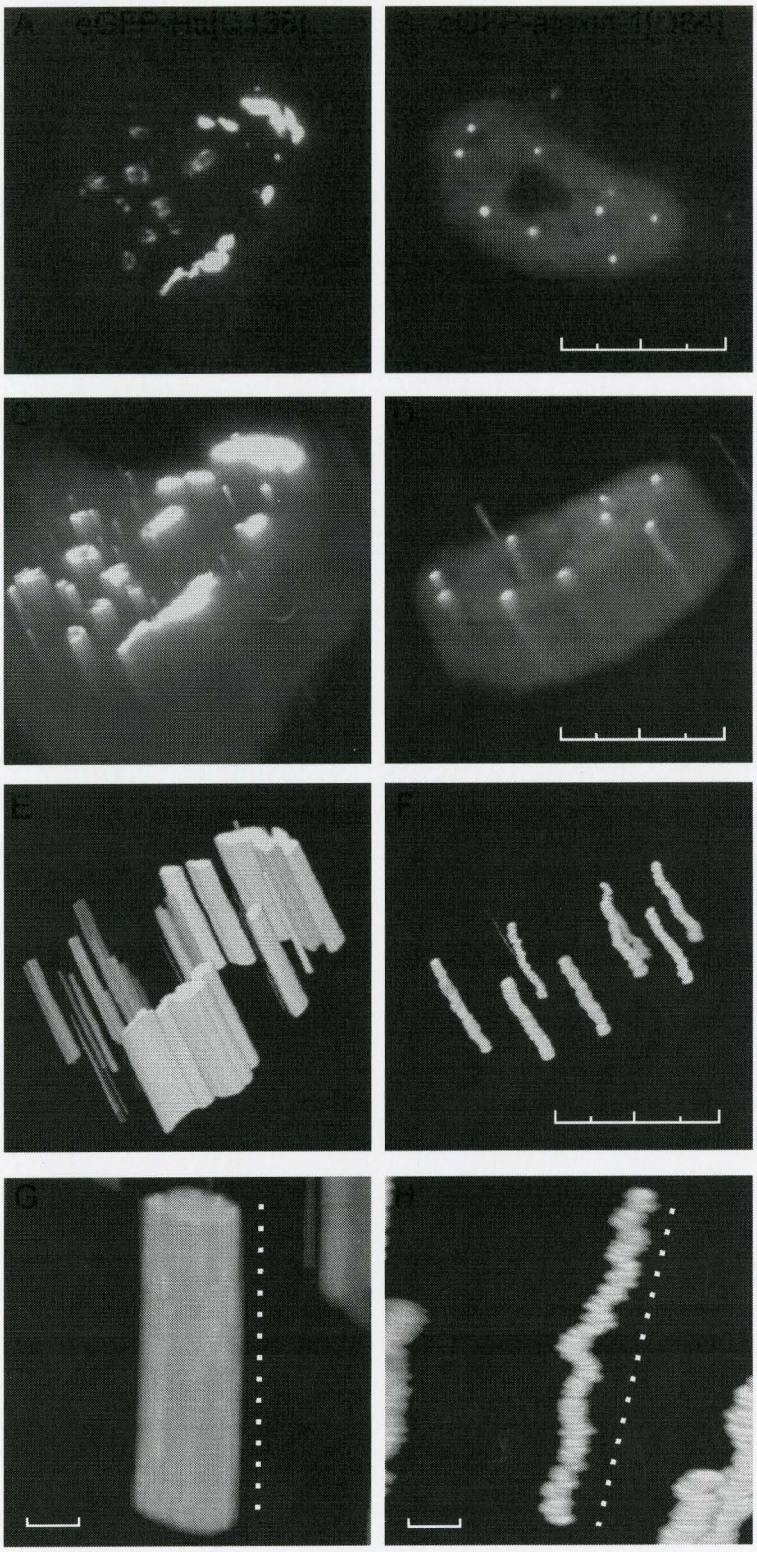

Figure 2

Figure 2. Ataxin-1 Nuclear Inclusions are Dynamic and Distinct From Huntingtin Polyglutamine Aggregates. Three-dimensional (x,y,time) analysis of huntingtin and ataxin-1 nuclear inclusions by live cell fluorescent video microscopy. Panels A and B, Fluorescence images of eGFP-huntingtin exon1 [Q138] and eGFP-ataxin-1 [Q84] video sequences captured at 0.5 second intervals for 30 seconds at 37°C. Panels C and D, x,y,t voxel images of time sequences in orthogonal view, intensities thresholded to inclusions only in Panels E and F. Panels G and H, three-dimensional single representative inclusions of huntingtin and ataxin-1 with dotted straight reference line. Scale bars in Panels A-F are 10 μm, 2 μm in Panels G,H. Also presented in Supplemental Videos 1 and 2. Hunting images captured by Ray Truant.

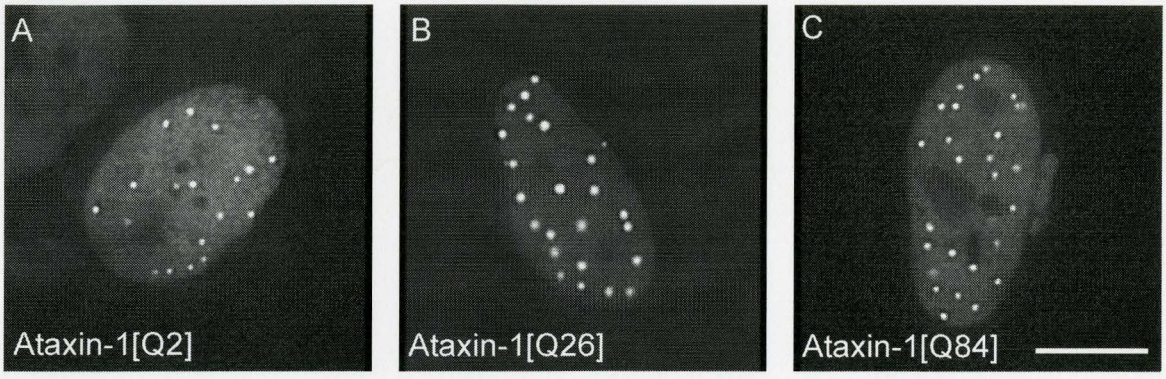

Figure 3

Figure 3. Ataxin-1 Nuclear Inclusion Formation and Movement are Not Dependent on Polyglutamine. Live cell fluorescence microscopy images of eGFP ataxin-1 [Q2] (Panel A), [Q26] (Panel B) or [Q84] (Panel C) at 37°C in Hela cells. Scale bar is 10um. Videos of inclusion movement for each ataxin-1 moiety are also presented as supplemental videos 3-5.

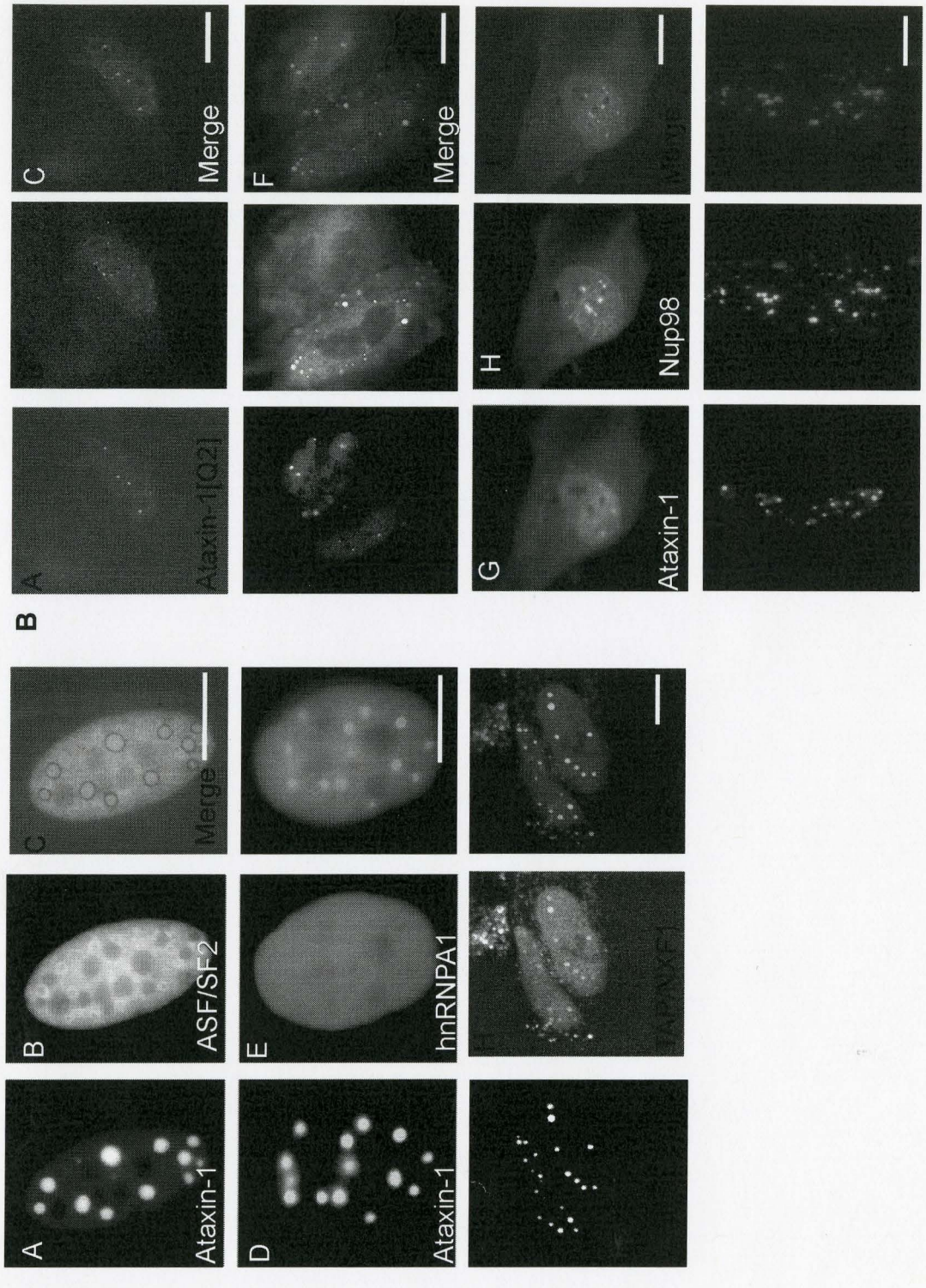
A
A
Ataxin-1
B
ASF/SF2
C
Merge
D
Ataxin-1
E
hnRNPA1
B
A
Ataxin-1[Q2]
C
Merge
F
G
Ataxin-1
H
Nup98

Figure 4

Figure 4: Ataxin-1 Nuclear Inclusions are Distinct From Other Nuclear Bodies. Live cell fluorescent patterns and dual channel overlay between ataxin-1 and known nuclear body proteins. Figure 4A, Panels A-C, eCFP-ataxin-1 [Q2] co-transfected with eYFP-ASF/SF2. Figure 4A, Panels D-F, eGFP-ataxin-1 [Q26] co-transfected with hnRNPA1-dsRed. Figure 4A, Panels G-1, laser confocal image of eCFP-ataxin-1 [Q2] co-transfected with mRFP-TAP/NXF1. Figure 4B, Panels A-C, eCFP-ataxin-1 [Q2] co-transfected with eGFP-gp210/TPR protein. Figure 4B, Panels D-F, eCFP-ataxin-1 [Q2] co-transfected with eGFP-huntingtin exon1 [Q138]. Figure 4B, Panels G-I, mRFP-ataxin-1 [Q2] co-transfected with eGFP- Nup98. Figure 6B, Panels J-L, eCFP-ataxin-1 [Q2] co-transfected with eGFP-promyelocytic leukemia (PML) protein. Scale bar is approximately 10 μm.

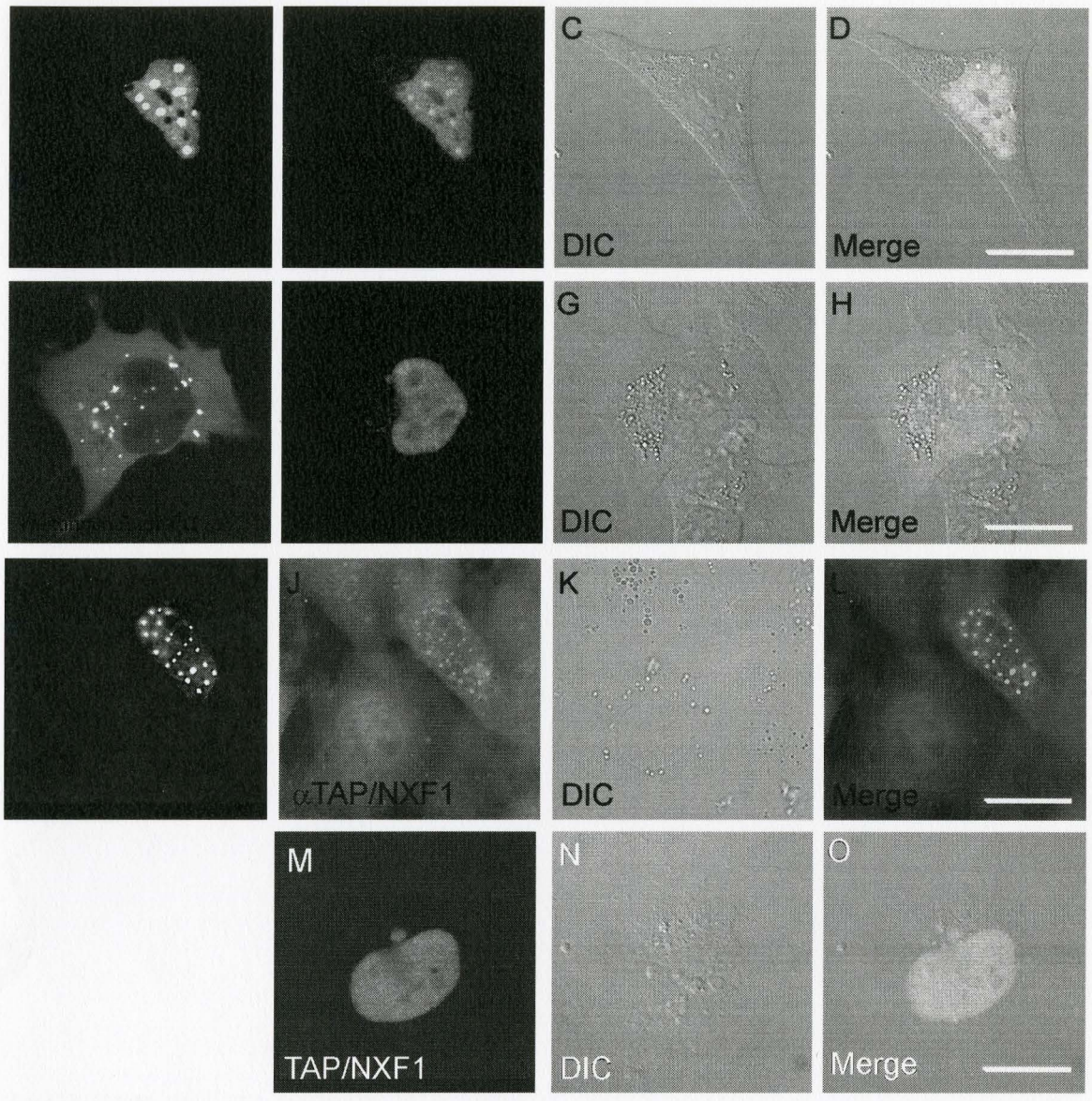
C
D
DIC
Merge
G
H
DIC
Merge
J
K
L
αTAP/NXF1
DIC
Merge
M
N
O
TAP/NXF1
DIC
Merge

Figure 5

Figure 5. Ataxin-1 Nuclear Inclusions Co-localize with TAP/NXF1 mRNA Export Factor. Laser confocal microscographs of eGFP-ataxin-1 [Q84] and mRFP-TAP/NXF1 (Panels A-D), huntingtin exon-1 [Q138] and mRFP-TAP/NXF1 (Panels E-H). Panels I-H show immunofluorescence micrographs captured by Ray Truant of TAP/NXF1 and ataxin-1 in HeLa cells. Panels M-O, mRFP-TAP/NXF1 transfected alone, displaying no punctate localization as in Panels D and L. Scale bar is approx. 10um.

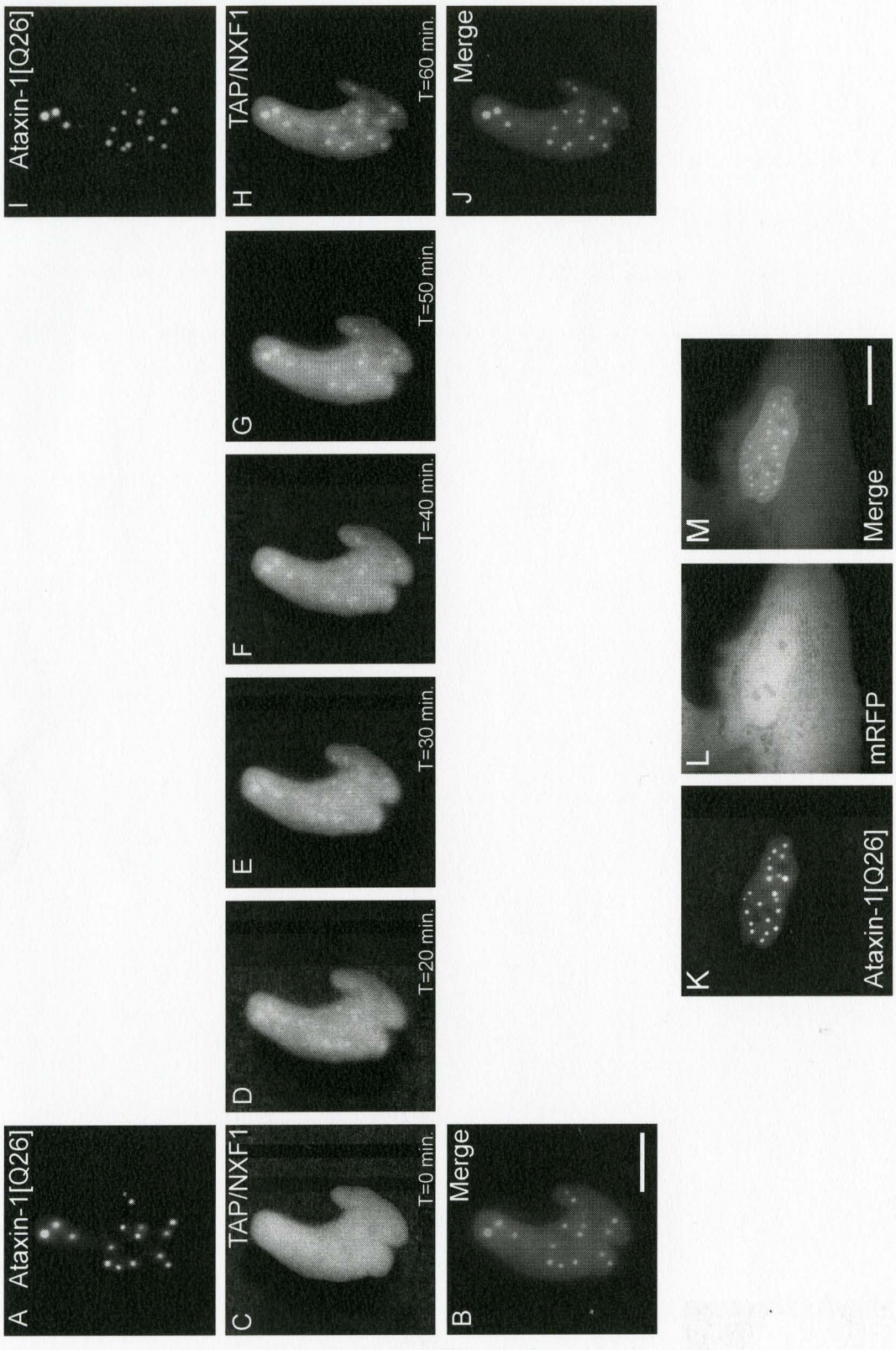
A Ataxin-1[Q26]
B Merge
C TAP/NXF1
T=0 min.
D
T=20 min.
E
T=30 min.
F
T=40 min.
G
T=50 min.
H TAP/NXF1
T=60 min.
I Ataxin-1[Q26]
J Merge
K
Ataxin-1[Q26]
L
mRFP
M
Merge

Figure 6

Figure 6. Ataxin-1 Recruits TAP/NXF1 Protein to Nuclear Inclusions as the Result of Cell Heat-shock. Fluorescence micrographs of eGFP-ataxin-1 [Q26] and mRFP-TAP/NXF1 in live cells before (Panels A-C) and after 42°C heat shock for five minutes, followed by incubation for one hour at 37°C (Panels I-J), with time course of TAP/NXF1 localization to ataxin-1 nuclear inclusions over 60 minutes in Panels C-H. Control of mRFP alone expressed with eGFP-ataxin-1 [Q26] after heat shock and one hour at 37°C in Panels K-M.

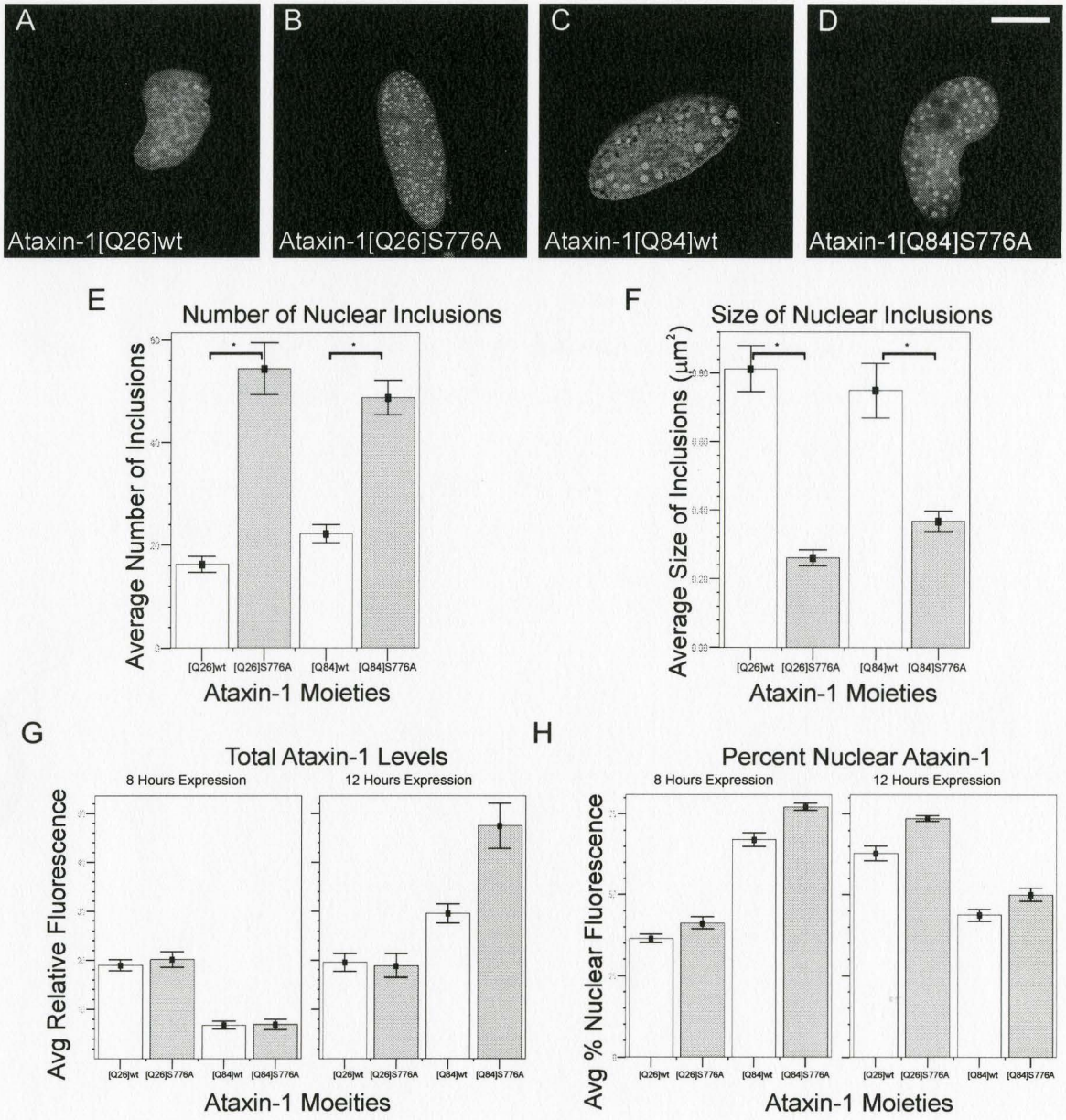
A
Ataxin-1[Q26]wt
B
Ataxin-1[Q26]S776A
C
Ataxin-1[Q84]wt
D
Ataxin-1[Q84]S776A
E
Number of Nuclear Inclusions
Average Number of Inclusions
[Q26]wt [Q26]S776A [Q84]wt [Q84]S776A
Ataxin-1 Moieties
F
Size of Nuclear Inclusions
Average Size of Inclusions (μm²)
[Q26]wt [Q26]S776A [Q84]wt [Q84]S776A
Ataxin-1 Moieties
G
Total Ataxin-1 Levels
8 Hours Expression
12 Hours Expression
Avg Relative Fluorescence
[Q26]wt [Q26]S776A [Q84]wt [Q84]S776A
Ataxin-1 Moeities
H
Percent Nuclear Ataxin-1
8 Hours Expression
12 Hours Expression
Avg % Nuclear Fluorescence
[Q26]wt [Q26]S776A [Q84]wt [Q84]S776A
Ataxin-1 Moieties

Figure 7

Figure 7. Quantitation of Ataxin-1 nuclear bodies, Total Fluorescence and Nuclear Localization of Ataxin-1, Unexpanded Versus Expanded Polyglutamine, Serine Versus Alanine at Position 776. Representative fluorescence micrographs of transiently transfected HeLa cells and quantitation of ataxin-1 properties. EGFP-ataxin-1 moieties are defined by either 26 or 84 glutamines per polyglutamine tract ([Q26] or [Q84]) and by either wild type or S776A point mutation (wt or S776A). (A-D), nuclei counterstained with Hoechst dye showing typical nuclear inclusions of ataxin-1 moieties, 12 hours post transfection. (E), average numbers of inclusions per ataxin-1 moiety. (F), average sizes of nuclear inclusions per ataxin-1 moiety in μm^2. (G), average total ataxin-1 expression levels by fluorescence intensity per ataxin-1 moiety at eight and 12 hours post-transfection. (H), average percent nuclear localization of ataxin-1 moieties by fluorescence intensity at eight and 12 hours post transfection. Error bars represent standard error. Asterisks indicate significant differences ($p<0.001$) for E and F. Images and graphs are representative of approximately 50 living cells per eGFP-ataxin-1 moiety.

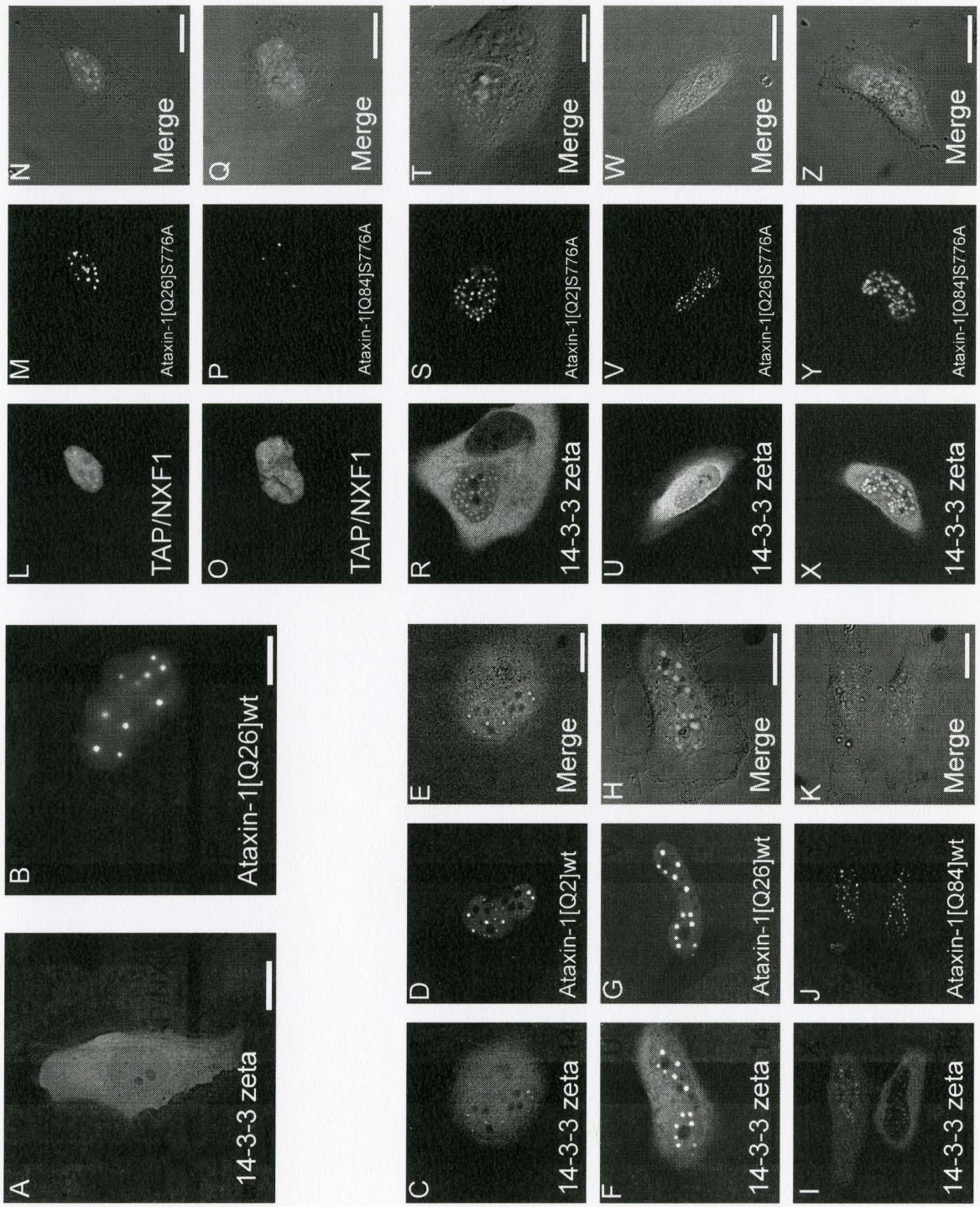
A
14-3-3 zeta
B
Ataxin-1[Q26]wt
C
14-3-3 zeta
D
Ataxin-1[Q2]wt
E
Merge
F
14-3-3 zeta
G
Ataxin-1[Q26]wt
H
Merge
I
14-3-3 zeta
J
Ataxin-1[Q84]wt
K
Merge
L
TAP/NXF1
M
Ataxin-1[Q26]S776A
N
Merge
O
TAP/NXF1
P
Ataxin-1[Q84]S776A
Q
Merge
R
14-3-3 zeta
S
Ataxin-1[Q2]S776A
T
Merge
U
14-3-3 zeta
V
Ataxin-1[Q26]S776A
W
Merge
X
14-3-3 zeta
Y
Ataxin-1[Q84]S776A
Z
Merge

Figure 8

Figure 8. 14-3-3 zeta is Present in Ataxin-1 nuclear bodies at Increased Local Concentrations Irrespective of Polyglutamine Expansion and S776A Mutation. Representative fluorescence (A, B) and laser confocal (C-Z) micrographs of transiently transfected HeLa cells. A-B, mRPF-14-3-3 zeta and eGFP-ataxin-1 [Q26] wt respectively. C-E, co-transfected mRFP-14-3-3 zeta and eGFP-ataxin-1 [2] wt. F-H, co-transfected mRFP-14-3-3 zeta and eGFP-ataxin-1 [Q26] wt. I-K, co-transfected mRFP-14-3-3 zeta and eGFP-ataxin-1 [Q84] wt. L-N, co-transfected mRFP-TAP/NXF1 and eGFP-ataxin-1 [Q26] S776A. O-Q, co-transfected mRFP-TAP/NXF1 and eGFP-ataxin-1 [Q84] S776A. R-T, co-transfected mRFP-14-3-3 zeta and eGFP-ataxin-1 [Q2] S776A. U-W, co-transfected mRFP-14-3-3 zeta and eGFP-ataxin-1 [Q26] S776A. X-Z, co-transfected mRFP-14-3-3 zeta and eGFP-ataxin-1 [Q84] S776A. Channel separations are as follows. A, C, F, I, L, O, R, U, X: mRFP. B, D, G, J, M, P, S, V, Y: eGFP. E, H, K, N, Q, T, W, Z: merged + DIC image.

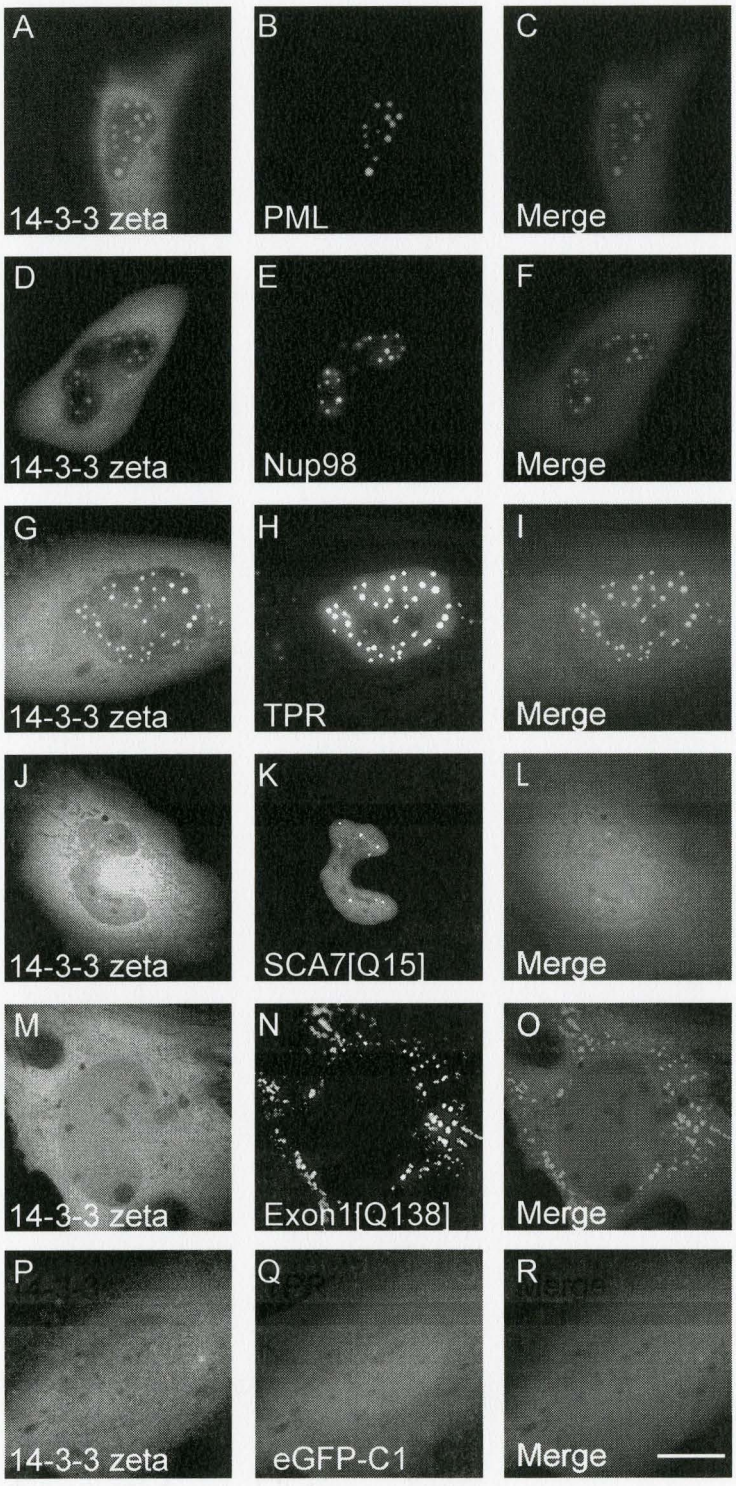
A
14-3-3 zeta
B
PML
C
Merge
D
14-3-3 zeta
E
Nup98
F
Merge
G
14-3-3 zeta
H
TPR
I
Merge
J
14-3-3 zeta
K
SCA7[Q15]
L
Merge
M
14-3-3 zeta
N
Exon1[Q138]
O
Merge
P
14-3-3 zeta
Q
eGFP-C1
R
Merge

Figure 9

Figure 9. 14-3-3 zeta Can be Found in Many Subnuclear Structures. Known inclusion forming fluorescent tagged protein constructs were co-expressed with mRPF-14-3-3 zeta and co-localization studies were performed on the resulting wide-field fluorescent micrographs. A-C, eGFP-PML. D-F, eGFP-Nup98. G-I, eGFP-gp210/TPR. J-L, SCA7. M-O, huntingtin exon-1 [Q138]. P-R, eGFP control. Panels A, D, G, J, M and P show mRFP 14-3-3 in an isolated channel. B, E, H, K, M and Q correspond to the eGFP channel. Panels C, F, I, L, O and P are the merged images.

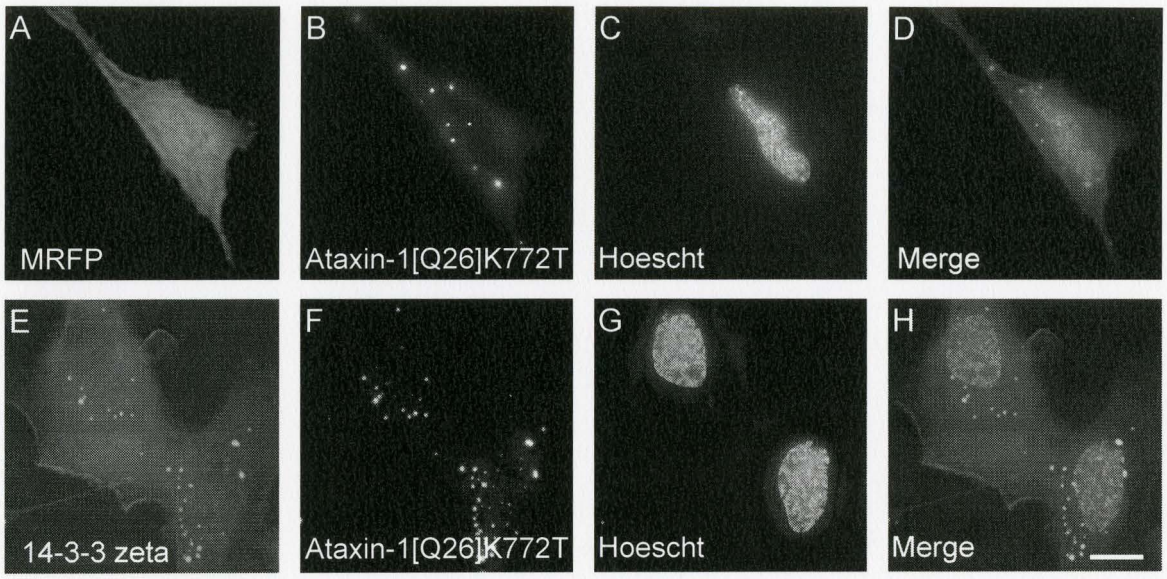
A
MRFP
B
Ataxin-1[Q26]K772T
C
Hoescht
D
Merge
E
14-3-3 zeta
F
Ataxin-1[Q26]K772T
G
Hoescht
H
Merge

Figure 10

Figure 10. Mutation of the Ataxin-1 NLS by Lysine to Threonine substitution at Position 772 Does Not Alter 14-3-3 Nucleocytoplasmic Distribution When Co-Expressed. Representative fluorescence micrographs of transiently transfected HeLa cells counterstained with Hoechst dye. A-D, eGFP-ataxin-1 [Q26]K772T co-transfected with mRFP control. E-H, eGFP-ataxin-1 [Q26]K772T co-transfected with mRFP-14-3-3 zeta. Channels are separated as follows. A, E: mRFP. B, F: eGFP. C, G: Hoechst. D, H: merged.

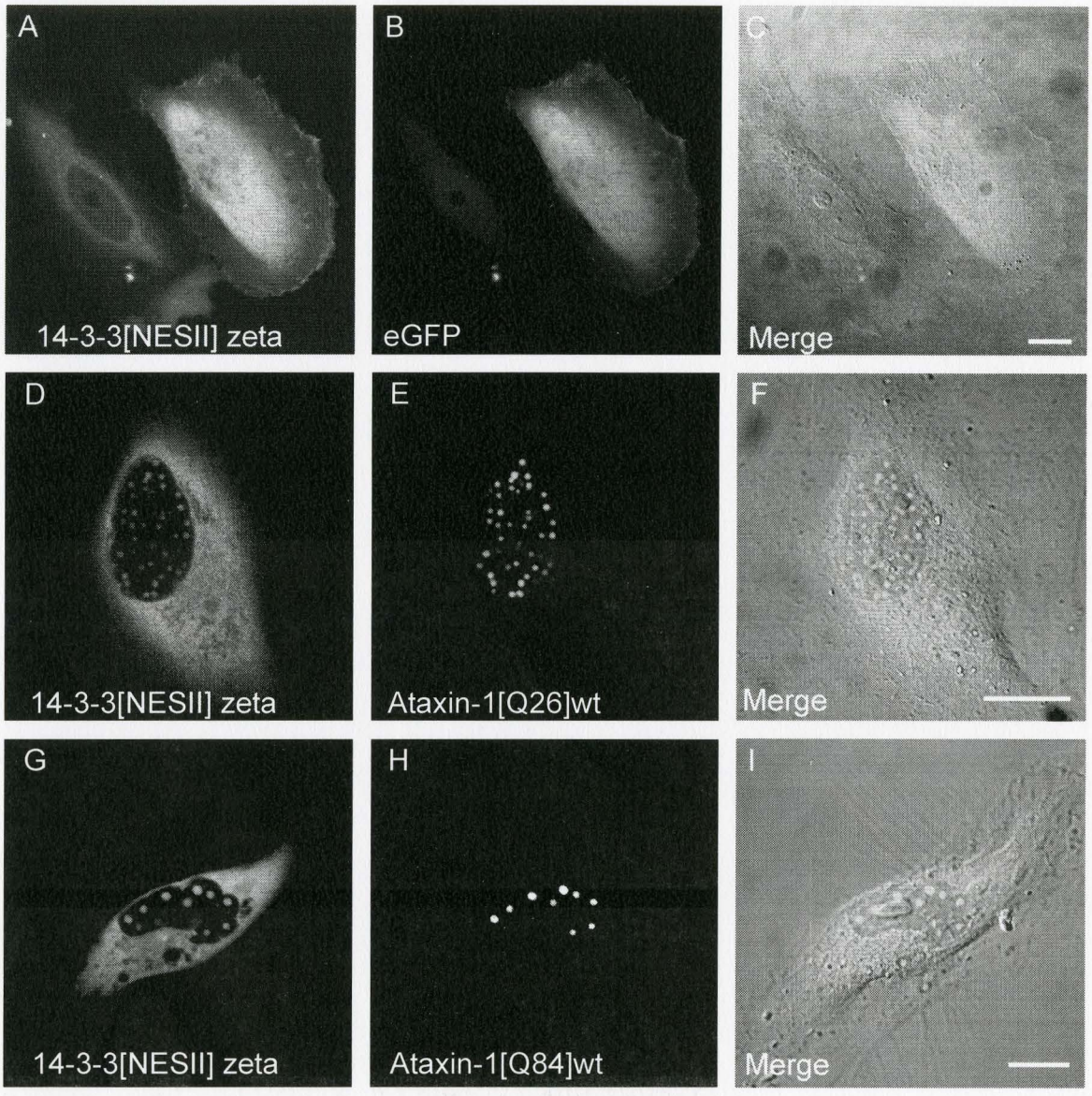
A
14-3-3[NESII] zeta
B
eGFP
C
Merge
D
14-3-3[NESII] zeta
E
Ataxin-1[Q26]wt
F
Merge
G
14-3-3[NESII] zeta
H
Ataxin-1[Q84]wt
I
Merge

Figure 11

Figure 11. Mutation of the 14-3-3 NES Does Not Sequester 14-3-3 zeta to the Nucleus in the Presence or Absence of Elevated Levels of Ataxin-1. Representative laser confocal fluorescence micrographs of transiently transfected HeLa cells. A-C, mRFP-14-3-3 [NESII] co-transfected with eGFP. D-F mRFP-14-3-3 [NESII] co-transfected with eGFP-ataxin-1 [Q26] wt. G-I mRFP-14-3-3 [NESII] co-transfected with eGFP-ataxin-1 [Q84] wt. Channels are separated as follows. A, D, G: mRFP. B, E, H: eGFP. C, F, I: merge + DIC.

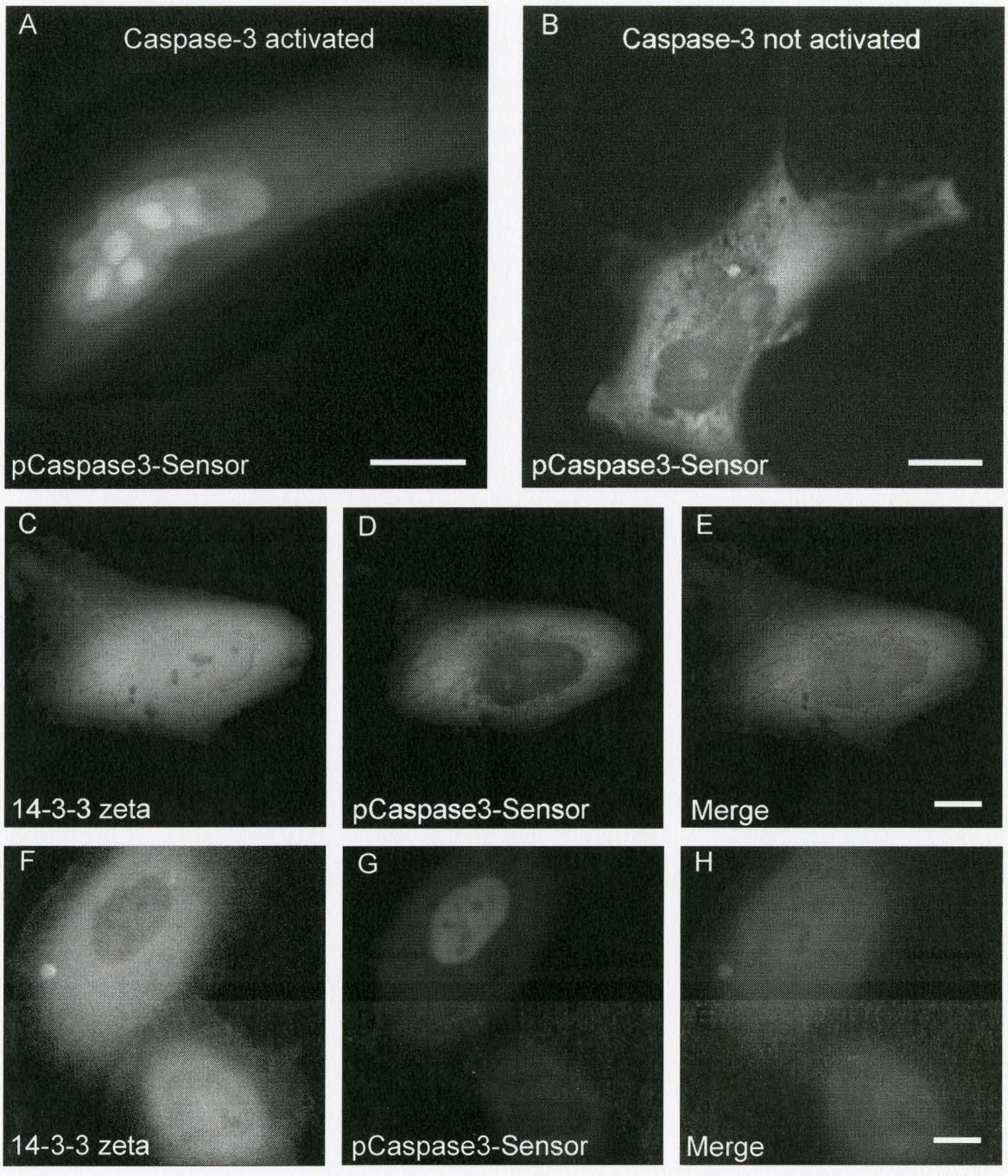
A
Caspase-3 activated
pCaspase3-Sensor
B
Caspase-3 not activated
pCaspase3-Sensor
C
14-3-3 zeta
D
pCaspase3-Sensor
E
Merge
F
14-3-3 zeta
G
pCaspase3-Sensor
H
Merge

Figure 12

Figure 12. 14-3-3 Does Not Enter the Nucleus in Response to Caspase-3 Mediated Apoptosis. Representative fluorescent micrographs of transiently transfected HeLa cells. pCaspase3-Sensor in (A) healthy and (B) caspase-3 activated cells are shown. C-E and F-H, co-transfected mRFP-14-3-3 zeta and pCaspase3p- Sensor in healthy and caspase-3 activated cells, respectively. Channels are separated as follows. C, F: mRFP. A, B, D, G: eGFP. E, H: merged.

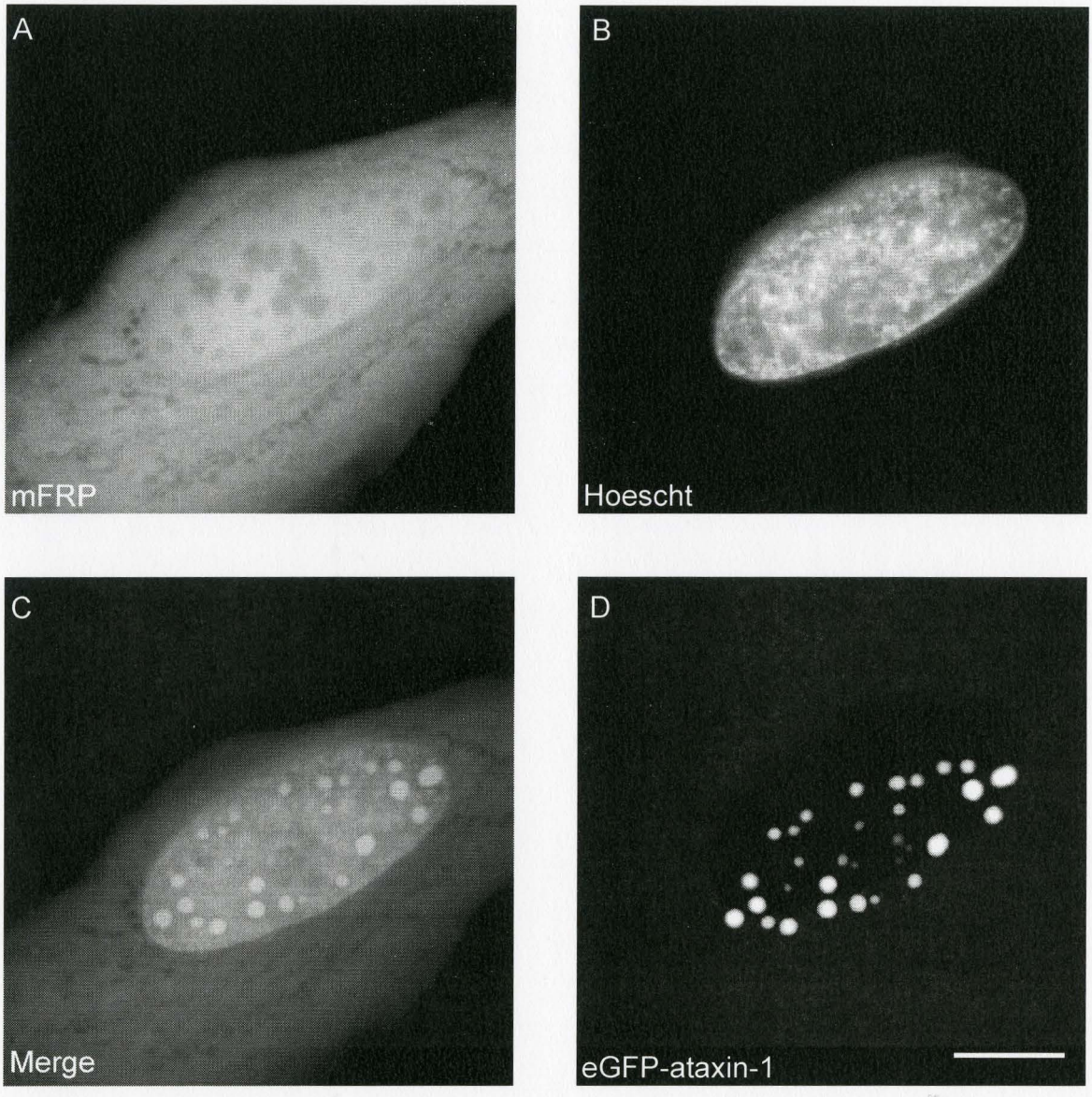

Figure 13

Figure 13. Self Blinded Selection. A self-blinding method used to reduce potential bias in selecting cells for quantitation. (A), Cells were first selected by viewing mRFP fluorescence only. Selection was made by arbitrarily assessing all cells for a similar level of red fluorescence. (B), the nucleus was then viewed for general roundness and was used as a point of reference for focus. All cells were focused to the centre of the nucleus. (C), The selected cell was then imaged according to preset parameters in the eGFP and Hoechst channels and the individually assigned parameters in the mRFP channel without viewing the eGFP image. Finally (D), the eGFP channel was used as an unbiased sample for measurement of intensity in the entire cell, the nucleus only and in the ataxin-1 nuclear bodies visible.

APPENDIX A

8.1 Self Blinded Selection of Cells

In any qualitative measurement, there is potential for sample bias. Data integrity is the responsibility of the experimenter, simple statistical methods do not take sample bias into consideration. This makes the assurance of unbiased sample collection at least as important as controlling experimental conditions between sample groups. For this reason, researchers often use methods of varying complexity which hide the identities of the samples being tested called blinding. While very effective, these methods can make data collection for large samples far less efficient than standard, or unblinded methods, and can become fiscally unfeasible for labs with limited resources. We have developed an effective, self blinded method for the collection of fluorescence micrographic data for our investigation of the nuclear localization of our eGFP-labelled ataxin-1 moieties.

Cells for selection and quantitation were transfected with both the cDNA of interest as an eGFP fusion and mRFP as a reporter or successful transfection, and to identify the outer limits of the cytoplasm. Counterstaining with Hoechst dye #33342 was used to identify the position and dimensions of the nucleus and to position the z-axis for imaging. Cells were screened subjectively using the Texas Red filterset only for mRFP function of an approximate minimum intensity. The exposure time was held constant at 0.556 ms and the Contrast Enhance Gain was adjusted up or down from five in order to ensure that the image was consistently bright but not overexposed. Once an appropriate cell was identified, the Hoechst filterset was used to focus on the centre of the nucleus to ensure a consistent Z position, with an exposure time of 100 ms to facilitate focusing and a Contrast Enhance Gain setting of 4.5 to ensure that the signal was of consistent brightness. Finally, the fluorescence micrograph was

taken of all three channels with the exposure time of interest using the GFP filterset, without having seen the green image. This three colour image was saved as a 48 bit RGB TIFF file for further analysis (Figure 13).

2.11 eGFP-ataxin-1 Moieties and Quantitation

Number of inclusions, size of inclusions, total fluorescence and average percent nuclear localization measurements were collected from the same cells which were allowed to express eGFP-ataxin-1 for 12 hours. Cells that expressed for only eight hours were used only for average percent nuclear localization and total fluorescence due to underdevelopment of inclusions at this short expression time. Fluorescent plasmid constructs were expressed, purified and quantitated using OD 280 at exactly the same time in order to reduce differences introduced by storage conditions. These constructs were then diluted to 500 ng/ul, quantitated an additional three times and averaged in order to obtain an accurate measurement. Samples with individual measurements deviating five percent or more from the mean were rejected and the sample was measured an additional three times. OD260/280 ratios were used as relative measures of DNA purity and were also measured three times and subjected to the same control. Samples with average ratios outside of the arbitrarily designated 1.80-1.86 window were rejected and the preparation of the plasmids was repeated until adequate purity of all constructs was achieved at the same time. HeLa cells from the same passage were split into four separate dishes and grown to 80-90% confluence. Each dish was used to seed 3, 25 mm glass-bottomed dishes to 140 000 cells as precisely as possible. These cells were transfected exactly four hours later with one μg of eGFP-ataxin-1 and 0.5 μg of mRFP and centrifuged

(Beckman Coulter Allegra 6 with GH 3.8 rotor) for one minute at 400 RPM using swinging buckets (Beckman Microplus carrier) with custom made plexiglass stabilizers that hold3, 25 mm tissue culture dishes each. Exactly seven or 11 hours later they were treated with Hoechst dye resulting in a final time of eight or 12 hours. Fluorescence microscopic imaging followed immediately for no more than 20 minutes per dish.

After random selection of cells, each cell was micrographed twice using the 60X objective with an unbinned capture resolution of 256x256 pixels, once with a 50 ms exposure in the eGFP channel for standardized measurement of fluorescence (set 1), and once with the eGFP exposure adjusted so that the images were of similar maximum brightness (set 2), using the histogram provided with image by Simple PCI. Images in the Hoechst and mRFP channels were unchanged between micrographs. This adjusted image was used to collect data on the ataxin-1 nuclear inclusions. Each image was contrast and brightness adjusted in both the red and blue channels so that the entire cell was represented by an intensity of 255 in the red channel, and the nucleus was represented by an intensity of 255 in the blue channel. The green channel was not adjusted in this procedure. These images were all saved as 24 bit RGB TIFF (tagged image file format) files for quantitation.

Adjusted 24 bit images were imported into Simple PCI as a single data document. Total cellular fluorescence, roundness, area, maximum intensity and minimum intensity were collected using the motion tracking analysis capabilities of Simple PCI. The "Identify" settings were as follows. Red: minimum (255), maximum (255). Blue and green channels were left unconstrained. The "modify" application was used for single passes of "full prune" and "fill holes". A minimum area of 500 μm^2 only using the "qualify" menu filtered out small pieces of other cells and small imaging artefacts. During data collection, problem cells were flagged for

possible exclusion. A problem cell was defined as one whose nucleus was incompletely stained with Hoechst dye, or that was obviously dead. A second pass of data collection was required for nuclear fluorescence. The "identify" menu was altered to select for areas with both red and blue intensities of 255, and the "qualify" menu was altered to select for only objects with a minimum area of 100 μm^2. The "runtime" menu allowed for Hoechst dye artefacts to be removed during data collection by adjusting exclusion criteria where needed. A third pass using set two was required in order to collect the data on the ataxin-1 nuclear inclusions. Identification requirements were red (255), blue (255) and green (100-255). The attribute "separate" was used only in this pass in order to separate nearly merged inclusions, and qualification required a minimum inclusion size of 100 nm^2. All three datasets were aligned so that each attribute measured was associated with a single record and saved.

REFERENCES

Alvarez, D., M. Callejo, R. Shoucri, L. Boyer, G. B. Price and M. Zannis-Hadjopoulos (2003). "Analysis of the cruciform binding activity of recombinant 14-3-3zeta-MBP fusion protein, its heterodimerization profile with endogenous 14-3-3 isoforms, and effect on mammalian DNA replication in vitro." Biochemistry **42**(23): 7205-15.

Bachi, A., I. C. Braun, J. P. Rodrigues, N. Pante, K. Ribbeck, C. von Kobbe, U. Kutay, M. Wilm, D. Gorlich, M. Carmo-Fonseca and E. Izaurralde (2000). "The C-terminal domain of TAP interacts with the nuclear pore complex and promotes export of specific CTE-bearing RNA substrates." Rna **6**(1): 136-58.

Banfi, S., A. Servadio, M. Chung, F. Capozzoli, L. A. Duvick, R. Elde, H. Y. Zoghbi and H. T. Orr (1996). "Cloning and developmental expression analysis of the murine homolog of the spinocerebellar ataxia type 1 gene (Sca1)." Hum Mol Genet **5**(1): 33-40.

Banfi, S., A. Servadio, M. Y. Chung, T. J. Kwiatkowski, Jr., A. E. McCall, L. A. Duvick, Y. Shen, E. J. Roth, H. T. Orr and H. Y. Zoghbi (1994). "Identification and characterization of the gene causing type 1 spinocerebellar ataxia." Nat Genet **7**(4): 513-20.

Banfi, S. and H. Y. Zoghbi (1994). "Molecular genetics of hereditary ataxias." Baillieres Clin Neurol **3**(2): 281-95.

Blencowe, B. J., J. A. Bowman, S. McCracken and E. Rosonina (1999). "SR-related proteins and the processing of messenger RNA precursors." Biochem Cell Biol **77**(4): 277-91.

Blevins, M. B., A. M. Smith, E. M. Phillips and M. A. Powers (2003). "Complex formation among the RNA export proteins Nup98, Rae1/Gle2, and TAP." J Biol Chem **278**(23): 20979-88.

Bodoor, K., S. Shaikh, P. Enarson, S. Chowdhury, D. Salina, W. H. Raharjo and B. Burke (1999). "Function and assembly of nuclear pore complex proteins." Biochem Cell Biol **77**(4): 321-9.

Bogerd, H. P., R. A. Fridell, R. E. Benson, J. Hua and B. R. Cullen (1996). "Protein sequence requirements for function of the human T-cell leukemia virus type 1 Rex nuclear export signal delineated by a novel in vivo randomization-selection assay." Mol Cell Biol **16**(8): 4207-14.

Brown, L. Y. and S. A. Brown (2004). "Alanine tracts: the expanding story of human illness and trinucleotide repeats." Trends Genet **20**(1): 51-8.

Brown, V., P. Jin, S. Ceman, J. C. Darnell, W. T. O'Donnell, S. A. Tenenbaum, X. Jin, Y. Feng, K. D. Wilkinson, J. D. Keene, R. B. Darnell and S. T. Warren (2001). "Microarray identification of FMRP-associated brain mRNAs and altered mRNA translational profiles in fragile X syndrome." Cell **107**(4): 477-87.

Brunet, A., F. Kanai, J. Stehn, J. Xu, D. Sarbassova, J. V. Frangioni, S. N. Dalal, J. A. DeCaprio, M. E. Greenberg and M. B. Yaffe (2002). "14-3-3 transits to the nucleus and participates in dynamic nucleocytoplasmic transport." J Cell Biol **156**(5): 817-28.

Burright, E. N., H. B. Clark, A. Servadio, T. Matilla, R. M. Feddersen, W. S. Yunis, L. A. Duvick, H. Y. Zoghbi and H. T. Orr (1995). "SCA1 transgenic mice: a model for

neurodegeneration caused by an expanded CAG trinucleotide repeat." Cell **82**(6): 937-48.

Bustamante, J. O., E. R. Michelette, J. P. Geibel, D. A. Dean, J. A. Hanover and T. J. McDonnell (2000). "Calcium, ATP and nuclear pore channel gating." Pflugers Arch **439**(4): 433-44.

Byrd, D. A., D. J. Sweet, N. Pante, K. N. Konstantinov, T. Guan, A. C. Saphire, P. J. Mitchell, C. S. Cooper, U. Aebi and L. Gerace (1994). "Tpr, a large coiled coil protein whose amino terminus is involved in activation of oncogenic kinases, is localized to the cytoplasmic surface of the nuclear pore complex." J Cell Biol **127**(6 Pt 1): 1515-26.

Calapez, A., H. M. Pereira, A. Calado, J. Braga, J. Rino, C. Carvalho, J. P. Tavanez, E. Wahle, A. C. Rosa and M. Carmo-Fonseca (2002). "The intranuclear mobility of messenger RNA binding proteins is ATP dependent and temperature sensitive." J Cell Biol **159**(5): 795-805.

Campbell, R. E., O. Tour, A. E. Palmer, P. A. Steinbach, G. S. Baird, D. A. Zacharias and R. Y. Tsien (2002). "A monomeric red fluorescent protein." Proc Natl Acad Sci U S A **99**(12): 7877-82.

Chai, Y., J. Shao, V. M. Miller, A. Williams and H. L. Paulson (2002). "Live-cell imaging reveals divergent intracellular dynamics of polyglutamine disease proteins and supports a sequestration model of pathogenesis." Proc Natl Acad Sci U S A **99**(14): 9310-5.

Chang, D. D. and P. A. Sharp (1989). "Regulation by HIV Rev depends upon recognition of splice sites." Cell **59**(5): 789-95.

Chen, H. K., P. Fernandez-Funez, S. F. Acevedo, Y. C. Lam, M. D. Kaytor, M. H. Fernandez, A. Aitken, E. M. Skoulakis, H. T. Orr, J. Botas and H. Y. Zoghbi (2003). "Interaction of akt-phosphorylated ataxin-1 with 14-3-3 mediates neurodegeneration in spinocerebellar ataxia type 1." Cell **113**(4): 457-68.

Chen, Y. W., M. D. Allen, D. B. Veprintsev, J. Lowe and M. Bycroft (2003). "The structure of the AXH domain of spinocerebellar ataxin-1." J Biol Chem.

Cormack, B. P., R. H. Valdivia and S. Falkow (1996). "FACS-optimized mutants of the green fluorescent protein (GFP)." Gene **173**(1 Spec No): 33-8.

Cronshaw, J. M., A. N. Krutchinsky, W. Zhang, B. T. Chait and M. J. Matunis (2002). "Proteomic analysis of the mammalian nuclear pore complex." J Cell Biol **158**(5): 915-27.

Cullen, B. R. (2000). "Connections between the processing and nuclear export of mRNA: evidence for an export license?" Proc Natl Acad Sci U S A **97**(1): 4-6.

Cummings, C. J., M. A. Mancini, B. Antalffy, D. B. DeFranco, H. T. Orr and H. Y. Zoghbi (1998). "Chaperone suppression of aggregation and altered subcellular proteasome localization imply protein misfolding in SCA1." Nat Genet **19**(2): 148-54.

Cummings, C. J. and H. Y. Zoghbi (2000). "Fourteen and counting: unraveling trinucleotide repeat diseases." Hum Mol Genet **9**(6): 909-16.

de Chiara, C., C. Giannini, S. Adinolfi, J. de Boer, S. Guida, A. Ramos, C. Jodice, D. Kioussis and A. Pastore (2003). "The AXH module: an independently folded domain common to ataxin-1 and HBP1." FEBS Lett **551**(1-3): 107-12.

DiFiglia, M., E. Sapp, K. O. Chase, S. W. Davies, G. P. Bates, J. P. Vonsattel and N. Aronin (1997). "Aggregation of huntingtin in neuronal intranuclear inclusions and dystrophic neurites in brain." Science **277**(5334): 1990-3.

Eberhart, D. E. and S. T. Warren (1996). "The molecular basis of fragile X syndrome." Cold Spring Harb Symp Quant Biol **61**: 679-87.

Emamian, E. S., M. D. Kaytor, L. A. Duvick, T. Zu, S. K. Tousey, H. Y. Zoghbi, H. B. Clark and H. T. Orr (2003). "Serine 776 of Ataxin-1 Is Critical for Polyglutamine-Induced Disease in SCA1 Transgenic Mice." Neuron **38**(3): 375-87.

Eskiw, C. H., G. Dellaire, J. S. Mymryk and D. P. Bazett-Jones (2003). "Size, position and dynamic behavior of PML nuclear bodies following cell stress as a paradigm for supramolecular trafficking and assembly." J Cell Sci **116**(Pt 21): 4455-66.

Fahrenkrog, B. and U. Aebi (2003). "The nuclear pore complex: nucleocytoplasmic transport and beyond." Nat Rev Mol Cell Biol **4**(10): 757-66.

Fermentas (Retrieved Jan 2004). Fermentas Web Site. http://www.fermentas.com/catalog/reagents/exgen500.htm

Fischer, U., J. Huber, W. C. Boelens, I. W. Mattaj and R. Luhrmann (1995). "The HIV-1 Rev activation domain is a nuclear export signal that accesses an export pathway used by specific cellular RNAs." Cell **82**(3): 475-83.

Fornerod, M., M. Ohno, M. Yoshida and I. W. Mattaj (1997). "CRM1 is an export receptor for leucine-rich nuclear export signals." Cell **90**(6): 1051-60.

Fribourg, S. and E. Conti (2003). "Structural similarity in the absence of sequence homology of the messenger RNA export factors Mtr2 and p15." EMBO Rep **4**(7): 699-703.

Fridell, R. A., R. E. Benson, J. Hua, H. P. Bogerd and B. R. Cullen (1996). "A nuclear role for the Fragile X mental retardation protein." Embo J **15**(19): 5408-14.

Frosst, P., T. Guan, C. Subauste, K. Hahn and L. Gerace (2002). "Tpr is localized within the nuclear basket of the pore complex and has a role in nuclear protein export." J Cell Biol **156**(4): 617-30.

Fu, H., R. R. Subramanian and S. C. Masters (2000). "14-3-3 proteins: structure, function, and regulation." Annu Rev Pharmacol Toxicol **40**: 617-47.

Garden, G. A., R. T. Libby, Y. H. Fu, Y. Kinoshita, J. Huang, D. E. Possin, A. C. Smith, R. A. Martinez, G. C. Fine, S. K. Grote, C. B. Ware, D. D. Einum, R. S. Morrison, L. J. Ptacek, B. L. Sopher and A. R. La Spada (2002). "Polyglutamine-expanded ataxin-7 promotes non-cell-autonomous purkinje cell degeneration and displays proteolytic cleavage in ataxic transgenic mice." J Neurosci **22**(12): 4897-905.

Grande, M. A., I. van der Kraan, B. van Steensel, W. Schul, H. de The, H. T. van der Voort, L. de Jong and R. van Driel (1996). "PML-containing nuclear bodies: their spatial distribution in relation to other nuclear components." J Cell Biochem **63**(3): 280-91.

Griffis, E. R., S. Xu and M. A. Powers (2003). "Nup98 localizes to both nuclear and cytoplasmic sides of the nuclear pore and binds to two distinct nucleoporin subcomplexes." Mol Biol Cell **14**(2): 600-10.

Harvey, R. J. and R. M. Napper (1991). "Quantitative studies on the mammalian cerebellum." Prog Neurobiol **36**(6): 437-63.

Ho, S. N., H. D. Hunt, R. M. Horton, J. K. Pullen and L. R. Pease (1989). "Site-directed mutagenesis by overlap extension using the polymerase chain reaction." Gene **77**(1): 51-9.

Hodel, M. R., A. H. Corbett and A. E. Hodel (2001). "Dissection of a nuclear localization signal." J Biol Chem **276**(2): 1317-25.

Hong, S., S. Ka, S. Kim, Y. Park and S. Kang (2003). "p80 coilin, a coiled body-specific protein, interacts with ataxin-1, the SCA1 gene product." Biochim Biophys Acta **1638**(1): 35-42.

Hong, S., S. J. Kim, S. Ka, I. Choi and S. Kang (2002). "USP7, a ubiquitin-specific protease, interacts with ataxin-1, the SCA1 gene product." Mol Cell Neurosci **20**(2): 298-306.

Horton, R. M., H. D. Hunt, S. N. Ho, J. K. Pullen and L. R. Pease (1989). "Engineering hybrid genes without the use of restriction enzymes: gene splicing by overlap extension." Gene **77**(1): 61-8.

Hoshino, M., K. Tagawa, T. Okuda and H. Okazawa (2004). "General transcriptional repression by polyglutamine disease proteins is not directly linked to the presence of inclusion bodies." Biochem Biophys Res Commun **313**(1): 110-6.

Howell, J. L. and R. Truant (2002). "Live-cell nucleocytoplasmic protein shuttle assay utilizing laser confocal microscopy and FRAP." Biotechniques **32**(1): 80-2, 84, 86-7.

Huang, S. and D. L. Spector (1992). "U1 and U2 small nuclear RNAs are present in nuclear speckles." Proc Natl Acad Sci U S A **89**(1): 305-8.

Huang, S. and D. L. Spector (1996). "Dynamic organization of pre-mRNA splicing factors." J Cell Biochem **62**(2): 191-7.

Huynh, D. P., H. T. Yang, H. Vakharia, D. Nguyen and S. M. Pulst (2003). "Expansion of the polyQ repeat in ataxin-2 alters its Golgi localization, disrupts the Golgi complex and causes cell death." Hum Mol Genet **12**(13): 1485-96.

Irwin, S., M. VanDelft, J. Howell, J. Graczyk, H. Y. Zoghbi, H. T. Orr and R. Truant (2004). "Altered Nucleocytoplasmic Shuttling of Mutant Ataxin-1." In Preparation For Journal of Biological Chemistry.

Johnson, M. T. and T. J. Ebner (2000). "Processing of multiple kinematic signals in the cerebellum and motor cortices." Brain Res Brain Res Rev **33**(2-3): 155-68.

Jun, L., S. Frints, H. Duhamel, A. Herold, J. Abad-Rodrigues, C. Dotti, E. Izaurralde, P. Marynen and G. Froyen (2001). "NXF5, a novel member of the nuclear RNA export factor family, is lost in a male patient with a syndromic form of mental retardation." Curr Biol **11**(18): 1381-91.

Katahira, J., K. Strasser, A. Podtelejnikov, M. Mann, J. U. Jung and E. Hurt (1999). "The Mex67p-mediated nuclear mRNA export pathway is conserved from yeast to human." Embo J **18**(9): 2593-609.

Katsuno, M., H. Adachi, M. Doyu, M. Minamiyama, C. Sang, Y. Kobayashi, A. Inukai and G. Sobue (2003). "Leuprorelin rescues polyglutamine-dependent phenotypes in a transgenic mouse model of spinal and bulbar muscular atrophy." Nat Med **9**(6): 768-73.

Kaytor, M. D. and H. T. Orr (2001). "RNA targets of the fragile X protein." Cell **107**(5): 555-7.

Keminer, O. and R. Peters (1999). "Permeability of single nuclear pores." Biophys J **77**(1): 217-28.

Klement, I. A., P. J. Skinner, M. D. Kaytor, H. Yi, S. M. Hersch, H. B. Clark, H. Y. Zoghbi and H. T. Orr (1998). "Ataxin-1 nuclear localization and aggregation: role in polyglutamine-induced disease in SCA1 transgenic mice." Cell **95**(1): 41-53.

Klockgether, T., R. Ludtke, B. Kramer, M. Abele, K. Burk, L. Schols, O. Riess, F. Laccone, S. Boesch, I. Lopes-Cendes, A. Brice, R. Inzelberg, N. Zilber and J. Dichgans (1998).

"The natural history of degenerative ataxia: a retrospective study in 466 patients." Brain **121 (Pt 4)**: 589-600.

Korsmeyer, S. J. (1999). "BCL-2 gene family and the regulation of programmed cell death." Cancer Res **59**(7 Suppl): 1693s-1700s.

Kousteni, S., F. Tura, G. E. Sweeney and D. P. Ramji (1997). "Sequence and expression analysis of a Xenopus laevis cDNA which encodes a homologue of mammalian 14-3-3 zeta protein." Gene **190**(2): 279-85.

Kovtun, I. V. and C. T. McMurray (2001). "Trinucleotide expansion in haploid germ cells by gap repair." Nat Genet **27**(4): 407-11.

Koyano, S., K. Iwabuchi, S. Yagishita, Y. Kuroiwa and T. Uchihara (2002). "Paradoxical absence of nuclear inclusion in cerebellar Purkinje cells of hereditary ataxias linked to CAG expansion." J Neurol Neurosurg Psychiatry **73**(4): 450-452.

Kramer, P. R., C. E. Pearson and R. R. Sinden (1996). "Stability of triplet repeats of myotonic dystrophy and fragile X loci in human mutator mismatch repair cell lines." Hum Genet **98**(2): 151-7.

Lee, M. S., M. Henry and P. A. Silver (1996). "A protein that shuttles between the nucleus and the cytoplasm is an important mediator of RNA export." Genes Dev **10**(10): 1233-46.

Leffers, H., P. Madsen, H. H. Rasmussen, B. Honore, A. H. Andersen, E. Walbum, J. Vandekerckhove and J. E. Celis (1993). "Molecular cloning and expression of the transformation sensitive epithelial marker stratifin. A member of a protein family that has been involved in the protein kinase C signalling pathway." J Mol Biol **231**(4): 982-98.

Legrain, P. and M. Rosbash (1989). "Some cis- and trans-acting mutants for splicing target pre-mRNA to the cytoplasm." Cell **57**(4): 573-83.

Lenzmeier, B. A. and C. H. Freudenreich (2003). "Trinucleotide repeat instability: a hairpin curve at the crossroads of replication, recombination, and repair." Cytogenet Genome Res **100**(1-4): 7-24.

Liu, D., J. Bienkowska, C. Petosa, R. J. Collier, H. Fu and R. Liddington (1995). "Crystal structure of the zeta isoform of the 14-3-3 protein." Nature **376**(6536): 191-4.

Longman, D., T. McGarvey, S. McCracken, I. L. Johnstone, B. J. Blencowe and J. F. Caceres (2001). "Multiple interactions between SRm160 and SR family proteins in enhancer-dependent splicing and development of C. elegans." Curr Biol **11**(24): 1923-33.

Lorenzetti, D., K. Watase, B. Xu, M. M. Matzuk, H. T. Orr and H. Y. Zoghbi (2000). "Repeat instability and motor incoordination in mice with a targeted expanded CAG repeat in the Sca1 locus." Hum Mol Genet **9**(5): 779-85.

Masters, S. C., R. R. Subramanian, A. Truong, H. Yang, K. Fujii, H. Zhang and H. Fu (2002). "Survival-promoting functions of 14-3-3 proteins." Biochem Soc Trans **30**(4): 360-5.

Matilla, A., B. T. Koshy, C. J. Cummings, T. Isobe, H. T. Orr and H. Y. Zoghbi (1997). "The cerebellar leucine-rich acidic nuclear protein interacts with ataxin-1." Nature **389**(6654): 974-8.

Matilla, A., E. D. Roberson, S. Banfi, J. Morales, D. L. Armstrong, E. N. Burright, H. T. Orr, J. D. Sweatt, H. Y. Zoghbi and M. M. Matzuk (1998). "Mice lacking ataxin-1 display learning deficits and decreased hippocampal paired-pulse facilitation." J Neurosci **18**(14): 5508-16.

Misteli, T., J. F. Caceres and D. L. Spector (1997). "The dynamics of a pre-mRNA splicing factor in living cells." Nature **387**(6632): 523-7.

Moore, B. and V. J. Oerez (1967). Physiological and Biochemical Aspects of Nervous Integration. Englewood Cliffs, NJ, Prentice Hall.

Moroianu, J. (1997). "Molecular mechanisms of nuclear protein transport." Crit Rev Eukaryot Gene Expr **7**(1-2): 61-72.

Morton, N. E., J. M. Lalouel, J. F. Jackson, R. D. Currier and S. Yee (1980). "Linkage studies in spinocerebellar ataxia (SCA)." Am J Med Genet **6**(3): 251-7.

Muratani, M., D. Gerlich, S. M. Janicki, M. Gebhard, R. Eils and D. L. Spector (2002). "Metabolic-energy-dependent movement of PML bodies within the mammalian cell nucleus." Nat Cell Biol **4**(2): 106-10.

Mushegian, A. R., D. E. Bassett, Jr., M. S. Boguski, P. Bork and E. V. Koonin (1997). "Positionally cloned human disease genes: patterns of evolutionary conservation and functional motifs." Proc Natl Acad Sci U S A **94**(11): 5831-6.

Muslin, A. J. and H. Xing (2000). "14-3-3 proteins: regulation of subcellular localization by molecular interference." Cell Signal **12**(11-12): 703-9.

Mutai, H., Y. Toyoshima, W. Sun, N. Hattori, S. Tanaka and K. Shiota (2000). "PAL31, a novel nuclear protein, expressed in the developing brain." Biochem Biophys Res Commun **274**(2): 427-33.

Nakamura, K., S. Y. Jeong, T. Uchihara, M. Anno, K. Nagashima, T. Nagashima, S. Ikeda, S. Tsuji and I. Kanazawa (2001). "SCA17, a novel autosomal dominant cerebellar ataxia caused by an expanded polyglutamine in TATA-binding protein." Hum Mol Genet **10**(14): 1441-8.

Nakielny, S., U. Fischer, W. M. Michael and G. Dreyfuss (1997). "RNA transport." Annu Rev Neurosci **20**: 269-301.

Okazawa, H., T. Rich, A. Chang, X. Lin, M. Waragai, M. Kajikawa, Y. Enokido, A. Komuro, S. Kato, M. Shibata, H. Hatanaka, M. M. Mouradian, M. Sudol and I. Kanazawa (2002). "Interaction between mutant ataxin-1 and PQBP-1 affects transcription and cell death." Neuron **34**(5): 701-13.

Okuda, T., H. Hattori, S. Takeuchi, J. Shimizu, H. Ueda, J. J. Palvimo, I. Kanazawa, H. Kawano, M. Nakagawa and H. Okazawa (2003). "PQBP-1 transgenic mice show a late-onset motor neuron disease-like phenotype." Hum Mol Genet **12**(7): 711-25.

Orr, H. T., M. Y. Chung, S. Banfi, T. J. Kwiatkowski, Jr., A. Servadio, A. L. Beaudet, A. E. McCall, L. A. Duvick, L. P. Ranum and H. Y. Zoghbi (1993). "Expansion of an unstable trinucleotide CAG repeat in spinocerebellar ataxia type 1." Nat Genet **4**(3): 221-6.

Orr, H. T. and H. Y. Zoghbi (2001). "SCA1 molecular genetics: a history of a 13 year collaboration against glutamines." Hum Mol Genet **10**(20): 2307-11.

Pante, N. and U. Aebi (1996). "Sequential binding of import ligands to distinct nucleopore regions during their nuclear import." Science **273**(5282): 1729-32.

Pante, N., R. Bastos, I. McMorrow, B. Burke and U. Aebi (1994). "Interactions and three-dimensional localization of a group of nuclear pore complex proteins." J Cell Biol **126**(3): 603-17.

Pante, N. and M. Kann (2002). "Nuclear pore complex is able to transport macromolecules with diameters of about 39 nm." Mol Biol Cell **13**(2): 425-34.

Pasquinelli, A. E., R. K. Ernst, E. Lund, C. Grimm, M. L. Zapp, D. Rekosh, M. L. Hammarskjold and J. E. Dahlberg (1997). "The constitutive transport element (CTE) of Mason-Pfizer monkey virus (MPMV) accesses a cellular mRNA export pathway." Embo J **16**(24): 7500-10.

Pearson, C. E. and R. R. Sinden (1996). "Alternative structures in duplex DNA formed within the trinucleotide repeats of the myotonic dystrophy and fragile X loci." Biochemistry **35**(15): 5041-53.

Perutz, M. (1994). "Polar zippers: their role in human disease." Protein Sci **3**(10): 1629-37.

Petosa, C., S. C. Masters, L. A. Bankston, J. Pohl, B. Wang, H. Fu and R. C. Liddington (1998). "14-3-3zeta binds a phosphorylated Raf peptide and an unphosphorylated peptide via its conserved amphipathic groove." J Biol Chem **273**(26): 16305-10.

Radu, A., M. S. Moore and G. Blobel (1995). "The peptide repeat domain of nucleoporin Nup98 functions as a docking site in transport across the nuclear pore complex." Cell **81**(2): 215-22.

Regad, T. and M. K. Chelbi-Alix (2001). "Role and fate of PML nuclear bodies in response to interferon and viral infections." Oncogene **20**(49): 7274-86.

Richards, R. I. and G. R. Sutherland (1992). "Dynamic mutations: a new class of mutations causing human disease." Cell **70**(5): 709-12.

Rittinger, K., J. Budman, J. Xu, S. Volinia, L. C. Cantley, S. J. Smerdon, S. J. Gamblin and M. B. Yaffe (1999). "Structural analysis of 14-3-3 phosphopeptide complexes identifies a dual role for the nuclear export signal of 14-3-3 in ligand binding." Mol Cell **4**(2): 153-66.

Ross, C. A. (1997). "Intranuclear neuronal inclusions: a common pathogenic mechanism for glutamine-repeat neurodegenerative diseases?" Neuron **19**(6): 1147-50.

Rossoll, W., A. K. Kroning, U. M. Ohndorf, C. Steegborn, S. Jablonka and M. Sendtner (2002). "Specific interaction of Smn, the spinal muscular atrophy determining gene product, with hnRNP-R and gry-rbp/hnRNP-Q: a role for Smn in RNA processing in motor axons?" Hum Mol Genet **11**(1): 93-105.

Saavedra, C., B. Felber and E. Izaurralde (1997). "The simian retrovirus-1 constitutive transport element, unlike the HIV-1 RRE, uses factors required for cellular mRNA export." Curr Biol **7**(9): 619-28.

Sankoh, A. J., M. F. Huque and S. D. Dubey (1997). "Some comments on frequently used multiple endpoint adjustment methods in clinical trials." Stat Med **16**(22): 2529-42.

Santos-Rosa, H., H. Moreno, G. Simos, A. Segref, B. Fahrenkrog, N. Pante and E. Hurt (1998). "Nuclear mRNA export requires complex formation between Mex67p and Mtr2p at the nuclear pores." Mol Cell Biol **18**(11): 6826-38.

Schlotterer, C. and D. Tautz (1992). "Slippage synthesis of simple sequence DNA." Nucleic Acids Res **20**(2): 211-5.

Schmitt, I. and L. Gerace (2001). "In vitro analysis of nuclear transport mediated by the C-terminal shuttle domain of Tap." J Biol Chem **276**(45): 42355-63.

Segref, A., K. Sharma, V. Doye, A. Hellwig, J. Huber, R. Luhrmann and E. Hurt (1997). "Mex67p, a novel factor for nuclear mRNA export, binds to both poly(A)+ RNA and nuclear pores." Embo J **16**(11): 3256-71.

Senay, C., P. Ferrari, C. Rocher, K. J. Rieger, J. Winter, D. Platel and Y. Bourne (2003). "The Mtr2-Mex67 NTF2-like domain complex. Structural insights into a dual role of Mtr2 for yeast nuclear export." J Biol Chem **278**(48): 48395-403.

Shahin, V., T. Danker, K. Enss, R. Ossig and H. Oberleithner (2001). "Evidence for Ca2+- and ATP-sensitive peripheral channels in nuclear pore complexes." Faseb J **15**(11): 1895-901.

Shen, Y. H., J. Godlewski, A. Bronisz, J. Zhu, M. J. Comb, J. Avruch and G. Tzivion (2003). "Significance of 14-3-3 self-dimerization for phosphorylation-dependent target binding." Mol Biol Cell **14**(11): 4721-33.

Shepherd, G. M. (1990). The Synaptic Oranization of the Brain. New York, Oxford University Press.

Siomi, H. and G. Dreyfuss (1995). "A nuclear localization domain in the hnRNP A1 protein." J Cell Biol **129**(3): 551-60.

Skinner, P. J., B. T. Koshy, C. J. Cummings, I. A. Klement, K. Helin, A. Servadio, H. Y. Zoghbi and H. T. Orr (1997). "Ataxin-1 with an expanded glutamine tract alters nuclear matrix-associated structures." Nature **389**(6654): 971-4.

Skinner, P. J., C. A. Vierra-Green, H. B. Clark, H. Y. Zoghbi and H. T. Orr (2001). "Altered trafficking of membrane proteins in purkinje cells of SCA1 transgenic mice." Am J Pathol **159**(3): 905-13.

Spector, D. L. (1996). "Nuclear organization and gene expression." Exp Cell Res **229**(2): 189-97.

Stenoien, D. L., M. Mielke and M. A. Mancini (2002). "Intranuclear ataxin1 inclusions contain both fast- and slow-exchanging components." Nat Cell Biol **4**(10): 806-10.

Takahashi, J., H. Fujigasaki, C. Zander, K. H. El Hachimi, G. Stevanin, A. Durr, A. S. Lebre, G. Yvert, Y. Trottier, H. The, J. J. Hauw, C. Duyckaerts and A. Brice (2002). "Two populations of neuronal intranuclear inclusions in SCA7 differ in size and promyelocytic leukaemia protein content." Brain **125**(Pt 7): 1534-43.

Takahashi, Y. (2003). "The 14-3-3 proteins: gene, gene expression, and function." Neurochem Res **28**(8): 1265-73.

Ule, J., K. B. Jensen, M. Ruggiu, A. Mele, A. Ule and R. B. Darnell (2003). "CLIP identifies Nova-regulated RNA networks in the brain." Science **302**(5648): 1212-5.

Vig, P. J., S. H. Subramony, Z. Qin, D. O. McDaniel and J. D. Fratkin (2000). "Relationship between ataxin-1 nuclear inclusions and Purkinje cell specific proteins in SCA-1 transgenic mice." J Neurol Sci **174**(2): 100-10.

Wang, X., N. Grammatikakis, A. Siganou and S. K. Calderwood (2003). "Regulation of molecular chaperone gene transcription involves the serine phosphorylation, 14-3-3 epsilon binding, and cytoplasmic sequestration of heat shock factor 1." Mol Cell Biol **23**(17): 6013-26.

Watase, K., E. J. Weeber, B. Xu, B. Antalffy, L. Yuva-Paylor, K. Hashimoto, M. Kano, R. Atkinson, Y. Sun, D. L. Armstrong, J. D. Sweatt, H. T. Orr, R. Paylor and H. Y. Zoghbi (2002). "A long CAG repeat in the mouse Sca1 locus replicates SCA1 features and reveals the impact of protein solubility on selective neurodegeneration." Neuron **34**(6): 905-19.

Weis, K. (2002). "Nucleocytoplasmic transport: cargo trafficking across the border." Curr Opin Cell Biol **14**(3): 328-35.

Wurtele, M., C. Jelich-Ottmann, A. Wittinghofer and C. Oecking (2003). "Structural view of a fungal toxin acting on a 14-3-3 regulatory complex." Embo J **22**(5): 987-94.

Xia, J., D. H. Lee, J. Taylor, M. Vandelft and R. Truant (2003). "Huntingtin contains a highly conserved nuclear export signal." Hum Mol Genet **12**(12): 1393-403.

Yue, S., H. G. Serra, H. Y. Zoghbi and H. T. Orr (2001). "The spinocerebellar ataxia type 1 protein, ataxin-1, has RNA-binding activity that is inversely affected by the length of its polyglutamine tract." Hum Mol Genet **10**(1): 25-30.

Zamanillo, D., R. Sprengel, O. Hvalby, V. Jensen, N. Burnashev, A. Rozov, K. M. Kaiser, H. J. Koster, T. Borchardt, P. Worley, J. Lubke, M. Frotscher, P. H. Kelly, B. Sommer, P. Andersen, P. H. Seeburg and B. Sakmann (1999). "Importance of AMPA receptors for hippocampal synaptic plasticity but not for spatial learning." Science **284**(5421): 1805-11.

Zenklusen, D. and F. Stutz (2001). "Nuclear export of mRNA." FEBS Lett **498**(2-3): 150-6.

Zenklusen, D., P. Vinciguerra, Y. Strahm and F. Stutz (2001). "The yeast hnRNP-Like proteins Yra1p and Yra2p participate in mRNA export through interaction with Mex67p." Mol Cell Biol **21**(13): 4219-32.

Zilliacus, J., E. Holter, H. Wakui, H. Tazawa, E. Treuter and J. A. Gustafsson (2001). "Regulation of glucocorticoid receptor activity by 14--3-3-dependent intracellular relocalization of the corepressor RIP140." Mol Endocrinol **15**(4): 501-11.

Zolotukhin, A. S. and B. K. Felber (1999). "Nucleoporins nup98 and nup214 participate in nuclear export of human immunodeficiency virus type 1 Rev." J Virol **73**(1): 120-7.